AEDC-TR-92-6

C.3

Development of a Laser-Induced Fluorescence System for Application to Rocket Plumes

C. W. Brasier and R. G. Porter
Sverdrup Technology, Inc., AEDC Group

January 1993

Final Report for Period October 1987 through April 1992

ARNOLD ENGINEERING DEVELOPMENT CENTER
ARNOLD AIR FORCE BASE, TENNESSEE
AIR FORCE MATERIEL COMMAND
UNITED STATES AIR FORCE

NOTICES

When U. S. Government drawings, specifications, or other data are used for any purpose other than a definitely related Government procurement operation, the Government thereby incurs no responsibility nor any obligation whatsoever, and the fact that the Government may have formulated, furnished, or in any way supplied the said drawings, specifications, or other data, is not to be regarded by implication or otherwise, or in any manner licensing the holder or any other person or corporation, or conveying any rights or permission to manufacture, use, or sell any patented invention that may in any way be related thereto.

Qualified users may obtain copies of this report from the Defense Technical Information Center.

References to named commercial products in this report are not to be considered in any sense as an endorsement of the product by the United States Air Force or the Government.

This report has been reviewed by the Office of Public Affairs (PA) and is releasable to the National Technical Information Service (NTIS). At NTIS, it will be available to the general public, including foreign nations.

APPROVAL STATEMENT

This report has been reviewed and approved.

David G. Burgess

DAVID G. BURGESS, Capt, USAF
Directorate of Technology
Deputy for Operations

Approved for publication:

FOR THE COMMANDER

Keith L Kushman

KEITH L. KUSHMAN
Director of Technology
Deputy for Operations

REPORT DOCUMENTATION PAGE

Form Approved
OMB No. 0704-0188

1 AGENCY USE ONLY (Leave blank)	2. REPORT DATE	3. REPORT TYPE AND DATES COVERED
	January 1993	Final Report for October 1987 - April 1992

4 TITLE AND SUBTITLE

Development of a Laser-Induced Fluorescence System for Application to Rocket Plumes

5. FUNDING NUMBERS

PE - 65807F

6. AUTHOR(S)

Brasier, C. W. and Porter, R. G.
Sverdrup Technology, Inc., AEDC Group

7 PERFORMING ORGANIZATION NAME(S) AND ADDRESS(ES)

Arnold Engineering Development Center/DOT
Air Force Materiel Command
Arnold Air Force Base, TN 37389-9011

8. PERFORMING ORGANIZATION REPORT NUMBER

AEDC-TR-92-6

9. SPONSORING/MONITORING AGENCY NAMES(S) AND ADDRESS(ES)

Arnold Engineering Development Center/DO
Air Force Materiel Command
Arnold Air Force Base, TN 37389-9010

10. SPONSORING/MONITORING AGENCY REPORT NUMBER

11. SUPPLEMENTARY NOTES

Available in Defense Technical Information Center (DTIC).

12a. DISTRIBUTION/AVAILABILITY STATEMENT

Approved for public release; distribution is unlimited.

12b DISTRIBUTION CODE

13. ABSTRACT (Maximum 200 words)

The status of a continuous wave scanning ring-dye laser-induced fluorescence system is presented. This system has been developed for measurements of velocity, temperature, pressure, and specie concentration in high-speed, high-temperature gas flows. Basic principles of laser-induced fluorescence of the sodium atom are discussed. Results of laboratory studies on a sodium vapor cell are presented. Application of this system to three full-scale liquid-propellant rocket engines is discussed, and initial results are presented.

14. SUBJECT TERMS	15. NUMBER OF PAGES
tunable dye laser, laser-induced fluorescence, velocity, temperature, pressure	48
	16. PRICE CODE

17. SECURITY CLASSIFICATION OF REPORT	18 SECURITY CLASSIFICATION OF THIS PAGE	19. SECURITY CLASSIFICATION OF ABSTRACT	20 LIMITATION OF ABSTRACT
UNCLASSIFIED	UNCLASSIFIED	UNCLASSIFIED	SAME AS REPORT

PREFACE

The work reported herein was conducted at Arnold Engineering Development Center (AEDC), Air Force Systems Command (AFSC), Arnold Air Force Base, Tennessee, and sponsored by the Director of Technology (DOT), AEDC. The applications reported in this work were conducted at the Stennis Space Center (SSC) Diagnostic Test Facility (DTF), sponsored by NASA/SSC; the NASA White Sands Test Facility, sponsored by SDIO/Phillips Labs; and the NASA Marshall Space Flight Center, (MSFC), sponsored by NASA/MSFC. The work was accomplished by Sverdrup Technology, Inc., AEDC Group, technical services contractor for the propulsion test facilities at the AEDC under Project Number DB87. The Air Force Project Manager was Capt. D. G. Burgess, and the Project Engineer was C. W. Brasier. The manuscript was submitted for publication on November 19, 1992.

CONTENTS

Page

1.0 INTRODUCTION 5
2.0 FLUORESCENCE THEORY 5
3.0 MEASUREMENT PARAMETERS USING LIF 8
4.0 SYSTEM DESCRIPTION 11
5.0 LABORATORY EXPERIMENTS 12
6.0 APPLICATIONS 13
6.1 Stennis Space Center (SCC) Diagnostic Test Facility (DTF) 13
6.2 Space Shuttle Orbital Maneuvering System (OMS) 14
6.3 Space Shuttle Main Engine (SSME) 15
7.0 FUTURE EFFORTS 17

REFERENCES 17

ILLUSTRATIONS

Figure Page

1. Sodium Atomic Structure 19
2. Structure of Sodium D1 and D2 Lines 20
3. Sodium Linewidth Versus Temperature 21
4. Sodium Linewidth Versus Pressure 22
5. Lineshape Distortion Due to Optical Pumping 23
6. Frequency Shift Versus Gas Velocity 24
7. Experimental Setup 25
8. Ring Laser Cavity 26
9. In-Line Reference Cell 27
10. Cross-Vapor Cell 27
11. Experimental Lineshape with Optical Pumping 28
12. Photograph of Diagnostic Test Facility 29
13. Schematic of Diagnostic Test Facility Layout 30
14. Photograph of Video Image of Sodium Fluorescence in DTF Plume 31
15. Fluorescence Profile at Axial Position of 1.5 in. 32
16. OMS LIF Installation 33
17. Photograph of OMS Laser System Setup 35
18. Photograph of Video Image of Sodium Fluorescence in OMS Plume 36
19. Sodium Fluorescence Distribution in OMS Plume 37

Figure Page

20. Laser Absorption and References 38
21. SSME Deck Area LIF System Installation 39
22. Photograph of Level 10 Area 40
23. Photograph of Level 10 Instrument Room 41

TABLES

1. Physical and Spectral Properties of Sodium Atoms 42
2. DTF LIF System Specifications 43
3. OMS LIF System Specifications 44
4. SSME LIF System Specifications 45

1.0 INTRODUCTION

Substantial progress has been made in the development of a laser-induced fluorescence (LIF) technique for nonintrusive gas diagnostics. A tunable dye laser system has been acquired, and operational skills developed providing a frequency-scannable light source for LIF. The system is currently being used for high-velocity gas flow diagnostics of plumes containing sodium atoms. The technique is expected to yield velocity, temperature, and pressure of the gas (Ref. 1). This technique is also applicable to the determination of specie concentrations and specie distributions in flames or exhaust flows.

This project has concentrated on developing both the experimental skills and understanding of LIF of the sodium (Na) atom using a tunable dye laser. In particular, laboratory experiments were conducted to experimentally verify the fluorescence characteristics of the sodium atom at various temperatures and buffer gas pressures. Measurements of the sodium fluorescence linewidth and absorption shift due to the buffer gas pressure and temperature were compared to theoretically predicted values.

In addition to the laboratory effort, an experimental evaluation of the LIF system has been conducted on liquid-propellant rocket plumes at the Stennis Space Center on the Diagnostic Test Facility (DTF), at the NASA White Sands Test Facility on a Space Shuttle Orbital Maneuvering System (OMS), and on the NASA Marshall Space Flight Center Technology Test Bed (TTB) Space Shuttle Main Engine (SSME).

This report presents a summary of important concepts associated with laser-induced fluorescence and initial results obtained in the laboratory and test stand applications.

2.0 FLUORESCENCE THEORY

Measurements of velocity, number density, temperature, and pressure are possible using LIF from atoms or molecules in a flowing gas such as the plume of a liquid-propellant rocket motor. To determine these parameters, the laser frequency is tuned through the resonant absorption frequency of the atom or molecule and, as a result, fluorescence emission occurs with the fluorescence signal recorded as a function of the laser frequency.

Although many species will fluoresce if they are illuminated with sufficient laser light of the correct frequency, species with near-ultraviolet and visible wavelength transitions are the easiest to work with. Listed below are some of the species that have been successfully measured with LIF.

Atoms	Diatomics	Polyatomics
Al	O_2	N_2O
B	H_2	S_2O_3
Ba	C_2	SO_2
Cl	OH	HCHO
H	CH	NCO
In	NO	NH_2
K	CN	
Mo	Cl_2	
Na	NH	
O		
Pb		
Si		
Tl		

AEDC efforts to date have concentrated on the use of the sodium atom as the fluorescing species for measurements in flow fields. Sodium is known to have a strong absorption cross section, thereby exhibiting strong fluorescence in the visible region. Sodium is naturally occurring in some high-temperature exhaust systems, thus eliminating the need to seed the flow via external means (Ref. 2).

Shown in Table 1 are properties of the sodium atom (Ref. 3).

Shown in Figs. 1 and 2 are the sodium atomic structure and the detailed structure of the D_1 and D_2 lines, respectively.

The D_1 ($3^2 S_{1/2}$ to $3^2 P_{1/2}$) line was used for the work reported here due to the ease of laser operation at this line. The respective cross sections of the sodium D-lines are given by:

$$\sigma(5890\text{Å}) = (10^{-12}\text{cm}^2)(8.037 - 1.31 \cdot 10^{-2}T + 2.30 \cdot 10^{-5}T^2) \quad (1)$$

$$\sigma(5896\text{Å}) = (10^{-12}\text{cm}^2)(3.968 - 6.40 \cdot 10^{-2}T + 1.11 \cdot 10^{-5}T^2) \quad (2)$$

where T is in °C (Ref. 4) and σ is the absorption cross section.

For low densities the fluorescence detected from a given region is proportional to the incident radiation absorbed in that region; therefore, absorption of the incident radiation as the beam propagates through the nondetected areas must be considered. The fluorescence from a given region is given by:

$$I_F = I_i - I_T = I_i[1 - \exp(-\sigma N L_{obs})]^{*}\gamma \quad (3)$$

where:

I_F = emitted fluorescence

I_i = incident laser radiation on the observation region

I_T = transmitted laser radiation

σ = absorption cross section

N = number density of sodium atoms

L_{obs} = observation length

γ = fluorescence efficiency as determined by the quenching of the sodium atoms

The irradiance I_i on the observation region is reduced from the incident irradiance I_o by the absorption prior to the observation region according to:

$$I_i = I_o \exp(-\sigma N L_{arm}) \quad (4)$$

where:

L_{arm} = length of vapor in the path of the laser beam prior to the observation region

I_o = incident laser radiation on the gas

The ratio of the fluorescence to the input irradiance is therefore:

$$I_F/I_o = \exp(-\sigma N L_{arm})[1 - \exp(-\sigma N L_{obs})] * \gamma \quad (5)$$

At low densities, the fluorescence increases linearly with the density, owing to the second factor in Eq. (5). At high densities, the fluorescence falls off exponentially, owing to the first factor. In between, a peak occurs at a unique value of N, given by:

$$N_{max} = (1/\sigma L_{obs}) \ell n((L_{arm} + L_{obs})/L_{arm}) \quad (6)$$

Given $L_{arm} >> L_{obs}$, Eq. (6) can be approximated as:

$$N_{max} = (1/(\sigma L_{arm})) \quad (7)$$

The sensitivity of the LIF technique for the measurement of velocity is determined from the linewidth of the emitted fluorescence. The natural linewidth of the sodium atom is 9.76 MHz, with a Doppler shift of 1.7 MHz for each meter per sec of flow velocity. The resolution of the resonant Doppler technique is limited to several meters per sec. The sodium linewidth is temperature and pressure broadened, with the thermal broadening given by:

$$\Delta\nu_t = 757(T/100)^{1/2}\text{MHz} \tag{8}$$

and with nitrogen or helium as the buffer gas, the pressure broadening is given by:

$$\Delta\nu_p = \delta_p(N/N_o)(T/100)^{1/2} + \delta_N\text{Hz} \tag{9}$$

where:

$\Delta\nu_t$ = FWHM due to thermal broadening

$\Delta\nu_p$ = FWHM due to pressure broadening

δ_p = $0.89 \cdot 10^{10}$ for N buffer gas

δ_p = $1.27 \cdot 10^{10}$ for He buffer gas

δ_N = $9.76 \cdot 10^6$ sodium natural linewidth

N_o = $2.69 \cdot 10^{19}$ molecules/cc

N = static number density of nitrogen

T = Temperature, °K

Shown in Fig. 3 is a plot of linewidth versus temperature. Figure 4 shows linewidth versus pressure. The pressure not only broadens the linewidth of the fluorescence profile, but also shifts the resonance line of the sodium atom. This shift in absorption frequency is to the red for nitrogen buffer gas and to the blue for helium, with the shifts given by:

$$\Delta\nu_{N_2} = -0.39 \cdot 10^{10}(N/N_o)(T/100)^{1/2} \tag{10}$$

$$\Delta\nu_{He} = 0.073 \cdot 10^{10}(N/N_o)(T/100)^{1/2} \tag{11}$$

where:

$\Delta\nu_{N_2}$ = resonant shift with N as buffer gas

$\Delta\nu_{He}$ = resonant shift with He as buffer gas

T = Temperature, °K

Lineshape distortion due to laser-induced optical pumping must be considered when the fluorescence profile is analyzed for either the determination of gas velocity from the shift in absorption frequency, or the determination of pressure from the width of the lineshape. The lineshape of the Na hyperfine doublet collapses to a single peak with an apparent frequency shift of the resonance line when the product of the laser power and buffer gas pressure exceeds approximately 0.1-mW torr (Ref. 5). With the gas velocity and pressure determination dependent on the frequency shift of the resonance line, any shift of this line due to optical pumping must be considered. Walkup (Ref. 5) has shown that the lineshape distortion is proportional to both incident laser power and the pressure. Examples of profile distortion as a function of laser power and pressure, as determined by Walkup, are shown in Fig. 5.

The absorption profile, A, is given by:

$$A = \frac{D[3/8R_1 + 5/8R_2] + R_1R_2}{D + 5/8R_1 + 3/8R_2}$$

where:

A = absorption profile

D = diffusion rate

R_1 = stimulated absorption rate

R_2 = stimulated absorption rate

Cancellation of the resonance shifts due to optical pumping and the shift due to pressure may be accomplished by utilization of a double-pass system using counter-propagating beams through the flow field (Ref. 6).

3.0 MEASUREMENT PARAMETERS USING LIF

Observation of LIF provides a means for the measurement of velocity, temperature, pressure, and specie concentration. Velocity measurements are relatively straightforward; however, temperature, pressure, and specie concentration are very dependent on gas pressures and chemistry effects. Corrections to the acquired data sets for these effects are beyond the scope of this report; therefore, only a cursory discussion of temperatures and pressure determinations will be presented.

The gas velocity along the laser beam is determined by the Doppler shift in the absorption frequency. The absorption frequency $\Delta\nu$ is given by:

$$\Delta\nu = \left(\frac{c}{c + Vg}\right)\nu_o - \nu_o \tag{13}$$

where:

$\Delta\nu$ = shifted absorption frequency

c = speed of light

V_g = velocity of the gas

ν_o = excitation frequency

A plot of the shift in the absorption frequency versus gas velocity is shown in Fig. 6. The fluorescence resulting from this shifted absorption may be compared to that of a stationary system, allowing the determination of the velocity component in the direction of the probe beam.

In addition to velocity, laser-induced fluorescence has also been used in a large number of ingenious ways to determine temperature, pressure, and specie concentration. Some of the more common LIF techniques are summarized below to give an indication of the versatility of the technique. Each measurement application has unique aspects and must be tailored to the particular target molecule or atom, and the nominal flow-field conditions.

Techniques utilized to obtain temperature from LIF measurements are the Perfect Gas Law, Internal State Distribution, and the Line Profile Methods. In flows where the pressure can be measured by a pitot probe or similar device, the temperature can be inverted from the Perfect Gas Law if the number density can be determined using LIF measurements. In flows where thermodynamic equilibrium is assured, the temperature of radical or molecular species can be determined from the ratio of fluorescence at different rotational or vibrational transitions. At low pressure, where the line profile is Doppler broadened, the temperature can be determined by a Gaussian fit to the LIF fluorescence line shape.

Pressure determination may be obtained by the Perfect Gas Law Method and the Line Profile Method. In flows where the temperature is known, the pressure is determined by the Perfect Gas Law provided a number density can be determined by LIF. At high pressure, where the line profile is Lorentzian, the pressure can be determined by a Lorentzian fit to the LIF fluorescence line shape.

Species concentration may be determined by saturated fluorescence and unsaturated fluorescence. In the case of saturated fluorescence, the fluorescent intensity is directly proportional to the target molecule concentration with sufficiently high laser power. For moderate to low laser power, the fluorescent intensity is reduced below the saturation level by quenching with the ambient gas molecules. (This fact leads to excellent high-contrast LIF

images of shocks and other pressure discontinuities.) In this case, reduction of the LIF signal to absolute species concentration requires knowledge of the ambient conditions.

4.0 SYSTEM DESCRIPTION

Shown in Fig. 7 is a schematic of the experimental setup used for the laboratory investigations of sodium fluorescence. The system consists of a Coherent 699-21 scanning ring dye laser pumped by a Spectra Physics Model 171-09 argon-ion laser. Using Rhodamine 6G laser dye and a pump laser power of 6 W at a wavelength of 5145 Å, the ring laser output is approximately 400 mW single frequency at a wavelength of 5896 Å. The frequency linewidth of the dye laser output is on the order of 500 kHz. Operation of the ring laser is very dependent on the power and mode quality of the pump laser. Included in the setup is laser diagnostic instrumentation which consists of a Burleigh wavemeter, model number WA-2000, and a Burleigh optical spectrum analyzer, model number SA-800. The wavemeter provides a convenient method of monitoring the laser wavelength during initial alignment and laser wavelength selection. The wavelength resolution of the wavemeter is on the order of 0.01 nm, which is insufficient to select the proper absorption wavelength, but does allow for rough wavelength alignment. A spectrum analyzer is also used to monitor the stability of the laser frequency. This spectrum analyzer is a confocal etalon with a frequency resolution of 40 MHz, which corresponds to a wavelength resolution of approximately 0.0005 nm and a free spectral range of 8 GHz.

The dye laser is operated so the output frequency is scanned ± 15 GHz about the peak absorption frequency of the sodium atom. This allows sufficient scanning range to adjust the laser frequency to the shifted absorption frequency of the sodium atoms. The scanning of the laser is accomplished with a piezoelectric mounted mirror in conjunction with a galvanometer-driven brewster plate located inside the laser cavity. A reference signal representing the laser frequency is supplied by the laser controller during the frequency scanning mode. A schematic of the ring laser cavity is shown in Fig. 8.

At the output of the dye laser, the beam is split so a portion of the beam is directed to the laser diagnostics and the sodium vapor reference cell with the remainder directed to the vapor cell on which the fluorescence measurements are made.

The fluorescence is detected using F1 optics and an RCA 8644 photomultiplier tube with S-20 photocathode. The output of the photomultiplier tube is displayed and stored on a digital storage oscilloscope.

The vapor cells are manufactured by Comstock, Inc., and consist of a stainless steel, 1-in.-ID tube whose length is large compared to its diameter (24 in.). The heater consists

of two "clamshell" ceramic halves containing coils of Nichrome® wire. The heater is insulated with a ceramic wool blanket and fiberglass tape. A type K thermocouple is embedded with refractory cement near the center of the heated tube and is used to monitor the tube temperature and to provide a feedback signal to regulate the temperatures. Sapphire windows were incorporated into both vapor cells. Figures 9 and 10 are dimensional drawings of both the inline reference cell and the cross cell used for the fluorescence measurements. A retractable mirror is positioned in front of the fluorescence cell so that incident laser power to the cell may be monitored.

The data acquisition system consists of a LeCroy Model 9400 digital oscilloscope interfaced to the microcomputer via a GPIB IEEE-488 interface. This interface provides programmable control of the oscilloscope functions and transfer of data from the oscilloscope to the microcomputer for data storage analysis. The oscilloscope functions are set to record the photodetector output of the reference cell photodiode, fluorescence signal from the photomultiplier tube from the sodium vapor cell, and the frequency scan reference from the laser controller. The storage scope is capable of storing up to a total of 64,000 eight-bit words before data transfer to the microcomputer is required. In addition to the digital scope, the signals are routed to a 16-channel Data Translation A/D board mounted inside the microcomputer.

5.0 LABORATORY EXPERIMENTS

Sodium fluorescence linewidth and absorption frequency measurements were made with the sodium vapor cell under various cell pressures and temperatures with nitrogen as the buffer gas. As noted earlier, the fluorescence was detected perpendicular to the direction of the laser beam. Approximately 0.25 gm of sodium was placed in the vapor cell. The temperature and pressure were varied as the linewidth and absorption frequency shift were recorded. The laser power was also varied to monitor lineshape as a function of laser power and pressure.

Measurements conducted in the laboratory on both absorption frequency shift with pressure and the fluorescence linewidth as a function of pressure and temperature were inconsistent with experiments previously conducted by Jongerius (Ref. 7). Disagreements on the order of a factor of two were seen in linewidth measurements as a function of temperature and pressure as compared to that of Jongerius. Measurements of the shift in absorption frequency as a function of pressure were also inconsistent with both the calculated values and experimental measurements of absorption shift as determined by both Miles and Jongerius. The calculated value of absorption shift is approximately 8.8 MHz per torr, as compared to our measurement of 4.0 to 6.5 MHz per torr. It should also be noted that the repeatability of the laboratory measurements was inconsistent.

The discrepancies in the data obtained are believed to be the result of optical pumping of the sodium atom as described by Walkup (Ref. 6). Measurements of the absorption profile with the laser power and pressure set such that the atom is in the optically pumped mode were made and showed good agreement with the predictions of Walkup. Shown in Fig. 11 are fluorescence profiles with the atom at various levels of laser power and pressure. This data set illustrates the effect of optical pumping on both the lineshape and the lineshift of the fluorescence profile.

Another concern is drift and/or a nonlinear scan of laser frequency as the laser frequency is scanned across the absorption profile of the sodium atom. Any drift in laser frequency from the apparent laser frequency would result in an error in the measurement of the absorption lineshift. Although these issues will ultimately have to be resolved, they do not impact the initial applications to flow-field visualization and velocity measurement in rocket exhausts. The system was, therefore, applied in its present state to several rocket tests.

6.0 APPLICATIONS

6.1 STENNIS SPACE CENTER (SSC) DIAGNOSTIC TEST FACILITY (DTF)

LIF was applied at the SSC on the DTF thruster engine to characterize its flow-field properties and evaluate the uniformity of the DTF seeding apparatus.

The DTF shown in Fig. 12 is a 1,200-lbf rocket engine fueled by gaseous hydrogen (GH_2) and liquid oxygen (LOX). It was designed and built for exhaust plume diagnostic sensor development and evaluation. The DTF is equipped with a plume-seeding device which allows precise amounts of seeding materials (dopants) to be injected into the combustion chamber. Using this unique capability, quantitative spectral analyses of Space Shuttle Main Engine (SSME) materials in the DTF exhaust plume are possible. No such plume seeding capability exists for the SSME.

The laser system consisted of the same components and layout as described earlier. The laser beam was routed to the test stand from the laser trailer via a 100-ft single-mode fiber-optic cable, delivering a collimated beam of approximately 2 mm in diameter and a laser power of approximately 70 mW. Detailed system specifications are given in Table 2. System layout relative to the test stand is shown in Fig. 13.

Video output of the LIF camera and the signal from the absorption photodiode were routed to recorders in the trailer. A CCD camera was used to monitor the status of the controlling electronics. The camera was pointed at the screens of the primary system diagnostics and the video was routed to the trailer housing the operating personnel. From this video

monitor, operating personnel could monitor proper operation of the equipment prior to engine ignition and during the motor firing. Both video and LIF data were acquired on 14 of the 17 firings of the DTF motor. Burn durations ranged from 6 to 27 sec. The O/F ratio for the 14 firings on which LIF data were obtained ranged from 4.65 to 5.41. Sodium concentrations at the nozzle exit plane were estimated to be on the order of 1 ppb.

The data obtained on the DTF plume consist of qualitative flow visualization provided by the sodium-filtered camera. This data set provides information on the positions of the plume boundary and nozzle-induced shock. Figure 14 is a photograph taken from a video image of the plume at the midpoint of the burn. The data obtained from the laser-induced fluorescence of sodium will provide information on the fuel distribution and relative radial velocity when the data analysis is completed. Shown in Fig. 15 is a profile of fluorescence intensity along the laser beam with the laser frequency tuned to the absorption frequency of the sodium atom. Quenching corrections are not incorporated in this data set. Therefore, the fluorescence profile is not necessarily proportional to the sodium concentration. This profile was obtained by digitizing a single video frame in which the laser frequency matches the sodium absorption frequency across the plume diameter. An intensity profile along the laser beam was then generated, representing the fluorescence intensity from the sodium atoms in the flow field. Note that with the laser scanning 30 GHz in 6 sec and a video framing rate of 30 Hz, the laser frequency scans approximately 166 MHz during a single video frame.

6.2 SPACE SHUTTLE ORBITAL MANEUVERING SYSTEM (OMS)

The LIF system was applied during a series of firings of the OMS liquid-propellant rocket engine at the NASA White Sands Test Facility.

Radial profiles of the fuel distribution in the OMS exhaust plume were obtained using laser-induced fluorescence (LIF) of trace amounts of the sodium impurity present in the fuel. The sodium D1 line, 0.5896 μm, was used as the probe line. An attempt was made to obtain radial profiles of the oxidizer using LIF of lithium, which was believed to be present in the oxidizer. The presence of lithium in the exhaust was not detectable by either the LIF system or an Optical Multichannel Analyzer system.

The laser system is the same as that described in Section 6.1. Table 3 contains the system specifications. The laser beam, approximately 3 mm in diameter, was directed across the plume centerline 4 in. below the nozzle exit plane. A CCD camera with a 54-in.-diam field of view was used as the detector. The camera lens was equipped with a 5-nm bandwidth line filter centered on the D1 line of the sodium atom. The video output of the camera was recorded on VHS tape. Measurements were also made of the laser power exiting the fiber-optic cable, the laser power transmitted through the plume, the laser frequency scan width, and the

fluorescence obtained from a fluorescence reference cell located on the optical table. Shown in Figs. 16a-b are schematics of the LIF installation in the test cell, and Fig. 17 is a photograph of the laser system setup as installed in the laser building located adjacent to the test cell.

Video data from the LIF system were obtained on ten of the fourteen motor firings. The video data from one of the OMS firings have been reviewed and compared to the laser absorption for the same laser scan during this firing. A photograph of a video image of the firing with sodium fluorescence is shown in Fig. 18. Shown in Fig. 19 is a fluorescence profile of a complete 30-GHz laser scan which has been corrected for the camera/filter response. This profile was obtained by digitizing all video frames with detectable fluorescence and then integrating the full data set to provide a single profile indicating relative sodium concentration across the plume. Note that the laser beam enters the plume at radial position 0 and exits the plume at radial position 50. From this profile, a decrease in the relative sodium concentration occurs on the beam exit side of the plume. Referring to the absorption profile taken on this same laser scan shown in Fig. 20, considerable absorption occurs when the laser frequency is near or on the absorption line of the sodium atom. It is not known at this time whether or not the reduced sodium level indicated in the integrated profile is due to absorption or possible beam movement on the detector caused by index of refraction variation in the plume at the sodium absorption line.

6.3 SPACE SHUTTLE MAIN ENGINE (SSME)

An experimental evaluation of laser-induced fluorescence (LIF) as applied to the SSME was conducted at the NASA Huntsville Technology Test Bed (TTB) facility. The purpose of this study was to determine the feasibility of acquiring LIF data to determine flow-field parameters on the SSME. Due to the high vibration levels during motor firings, there was great concern as to whether or not the laser systems could maintain optical alignment and single frequency operation during the SSME firings. To ensure operation during a motor firing, two complete scanning ring-dye laser systems were set up in the instrument room of Level 10, and the laser beams were routed to the test area via fiber-optic cables. Shown in Figs. 21 and 22 are the Level 10 deck area system installation. With concentrations of approximately 0.5 ppb expected in the flow, it was determined to utilize sodium as the fluorescing species. Both laser systems were tuned to the sodium D1 line, 0.5896 μm.

The laser systems are both the same as that described in Section 4.0. A photograph of the laser system setup as installed in the instrument room of Level 10 is shown in Fig. 23.

The frequency-scanned dye laser outputs were coupled to 100-ft optical fibers on the optical bench and routed to the Level 10 engine deck, with power outputs of approximately 80 mW each. From one laser system, a collimated beam of approximately 1.5 in. in diameter was

generated from the fiber-optic output and directed across the motor centerline approximately 3.5 in. downstream of the nozzle exit plane, while from the second laser system a beam of approximately 2.0 in. in diameter was generated and directed approximately 13.5 in. downstream of the nozzle exit plane. Three cameras viewing perpendicularly to the laser beams were used to view the beams at the motor centerline: a Xybion Model 250 intensified CCD camera, an RCA Model TC1030/H24 SIT camera, and a Dage Model CCD 72 CCD camera. All three cameras were equipped with 5-nm optical bandpass filters centered at the D1 sodium line. The Xybion field of view was approximately 48 in. and viewed the motor centerline to the edge of the plume; the Dage and RCA had fields of view of approximately 99 in., providing full exit plane viewing. All three camera views were tilted toward the top of the motor to avoid having the Mach disk within the camera viewing area. The output of each camera was recorded on video tape for posttest analysis. Time reference was obtained by recording IRIG time on the videotape.

The laser beam terminated on a photodiode mounted on the opposite side of the test cell to monitor laser beam absorption versus laser frequency. This was to provide a measure of whether or not the plume was optically thin. System specifications are summarized in Table 4.

During this test program, three SSME firings were conducted: two 205-sec burns and one 46-sec burn. Laser-induced fluorescence of the sodium in the engine exhaust was not observed on any of the three firings. This is believed to be due to a combination of low sodium concentration and insufficient laser beam power densities. It was learned in this technology development program that the laser systems will maintain optical alignment and single frequency operation throughout the full motor firing. This was verified via the system health monitor located in the control room. The laser was somewhat noisy, but reference fluorescence indicated laser stability was sufficient to tune on and off the absorption line of sodium. All three cameras survived all motor firings, but the video was saturated during the first motor firing due to sunlight reflection off the structure and the vapor cloud. To eliminate light scatter off the vapor cloud and structure, a tarp was placed as a viewing dump for the video cameras for the second and third firings. This appeared to provide sufficient blockage of the sunlight and provided a good, dark background for the video cameras. Even with the reduced background on the video cameras, there was no visible fluorescence detected on the final two motor firings. There was sufficient vibration on all firings of the fiber-optic output assembly such that the beam alignment on the absorption detector was lost at motor ignition. Review of the video obtained by the Xybion camera indicates that the laser beam position was still near the nozzle centerline. This was determined by observing particulate scatter of the laser beam from the purge gas through the nozzle after shutdown.

Since fluorescence from the sodium in the flow was not detected with the system geometry described, the laser beam energy density in the flow field should be increased in future testing. The optimum approach would be to direct the beam via mirrors to the test area to maintain a small beam diameter. This would increase the total laser power available to approximately

400 to 500 mW, a factor of 5 to 6 in laser power. Using the raw laser beam and natural divergence of the beam, the beam diameter will be reduced from 2.0 to 0.5 in. With the combination of increased laser power through the elimination of the fiber-optic cable and the reduced beam diameter, it is anticipated that the beam energy in the plume would increase by a factor of about 20.

7.0 FUTURE EFFORTS

Future experiments are planned to account for the inconsistencies in the laboratory data. The emphasis will be directed to acquiring data with sufficiently low laser powers and pressures to prevent lineshape distortion and absorption lineshift due to optical pumping of the atom. A flat-plate Fabry-Perot will be incorporated in the dye-laser diagnostics with sufficient free spectral range to monitor both the frequency scan range and scan linearity of the laser as it is scanned across the absorption profile of the sodium atom.

When appropriate funding is received, a detailed data analysis effort will be conducted on the data sets obtained on the DTF and OMS test programs. These data will be used to determine fuel distributions and radial velocity components in the plane of the laser beam. Provided the LIF data are of sufficient quality, analysis will also be conducted to obtain exhaust temperatures along the laser beam. Future experiments in applying a modified LIF system to the SSME are also being planned.

REFERENCES

1. Miles, R. B. "Resonant Doppler Velocimeter." *Physics of Fluids*, Vol. 18, No. 6, June 1975, p. 751.

2. Schmidt, E. W. *Hydrazine and Its Derivatives*. John Wiley & Sons, New York, 1984.

3. Cheng, Shi-Wai S. Thesis—"Resonant Doppler Velocimetry in Supersonic Nitrogen Flow." Princeton University, 1982. Also final report on NAG1-152, NASA-LR-169330 (NASA Langley).

4. Fairbank, W. M., Hansch, T. W., and Schalow, A. L. "Absolute Measurement of Very Low Sodium-Vapor Densities Using Laser Resonance Fluorescence." *Journal of the Optical Society of America*. Vol. 65, No. 2, February 1975, p. 199.

5. Walkup, R., Spielfiedel, A., Phillips, W. D., and Pritchard, D. E. "Line-Shape Changes Due to Optical Pumping of Na in Buffer Gas." *Physical Review A: General Physics* Vol. 23, No. 4, April 1981, p. 1869.

7. Jongerius, M. J., Van Bergen, A. R. D., Hollander, R. J., and Alkemade, C. Th. J. "An Experimental Study of the Collisional Broadening of the Na-D Lines by Ar, N2 and H_2 Perturbers in Flames and Vapor Cells-I." *Journal of Quantitative Spectroscopy and Radiative Transfer*, Vol. 25, 1981, pp. 1-18.

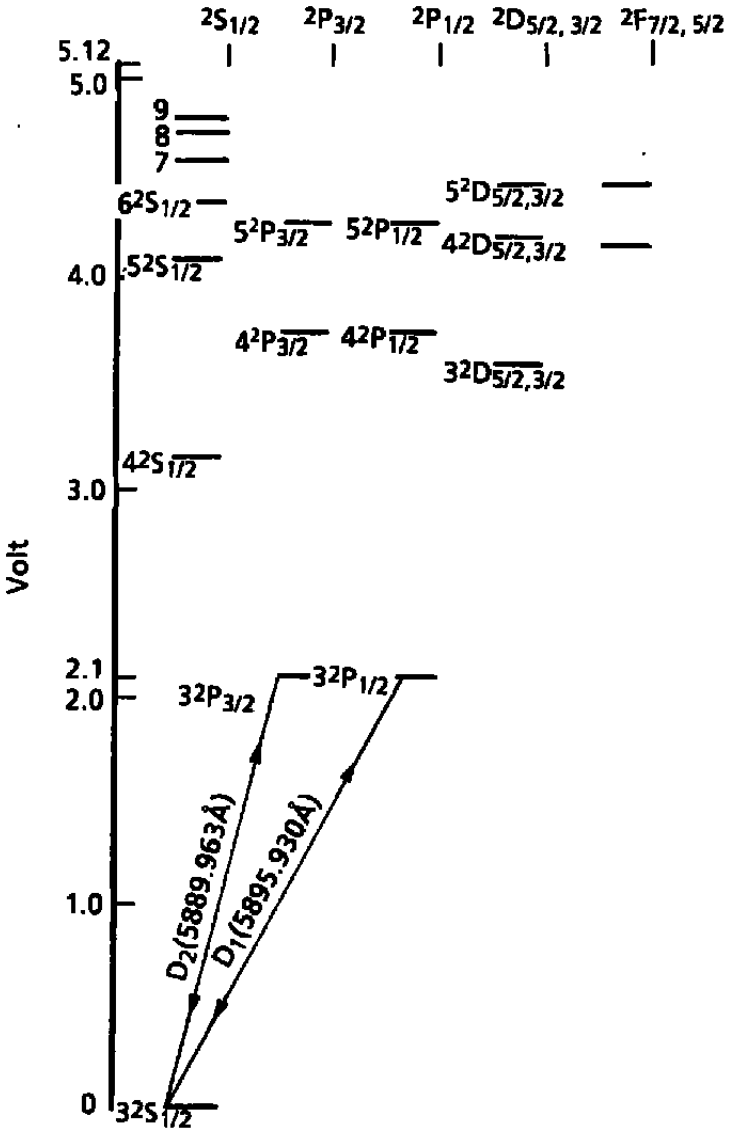

Figure 1. Sodium atomic structure.

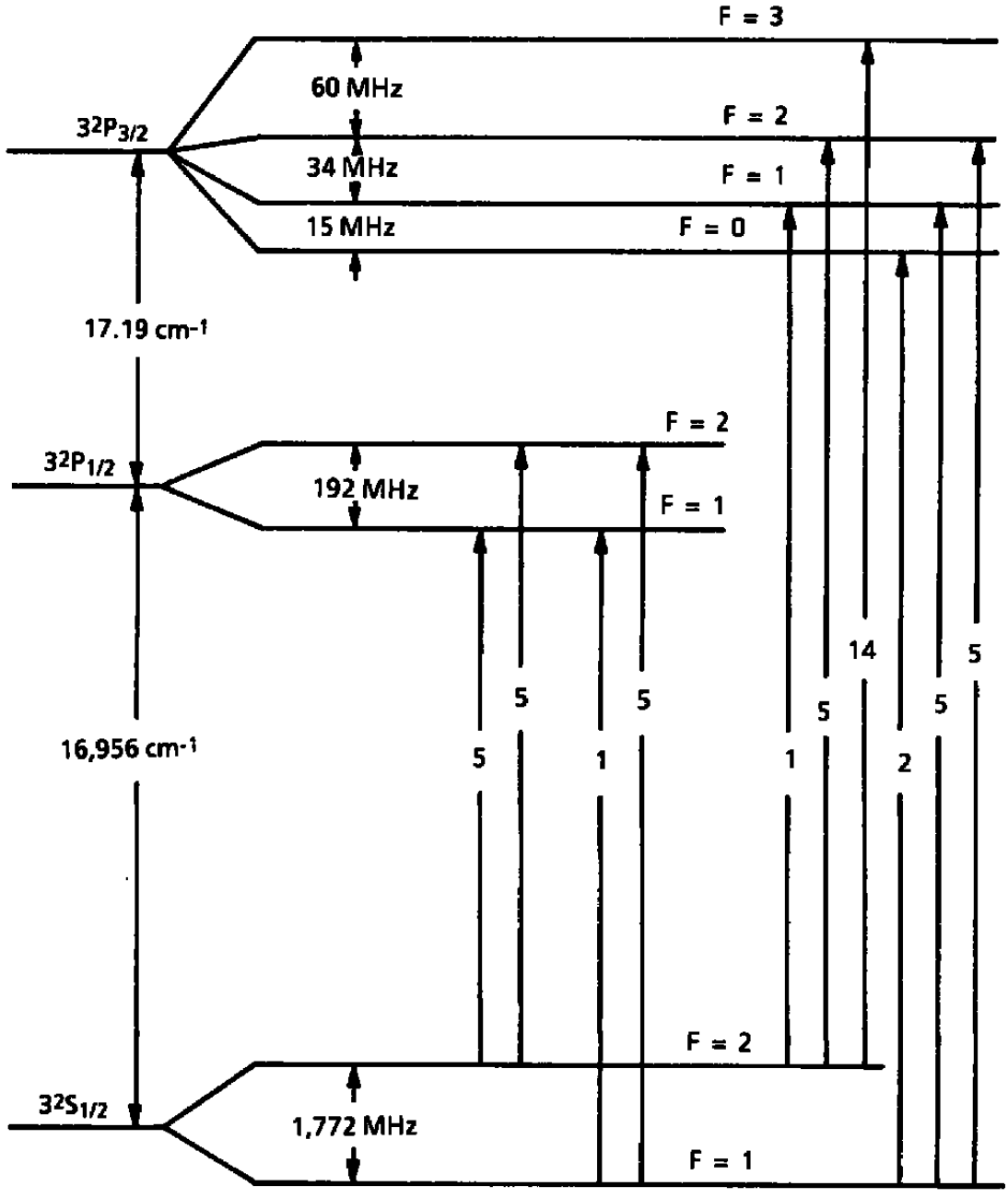

Figure 2. Structure of sodium D_1 and D_2 lines.

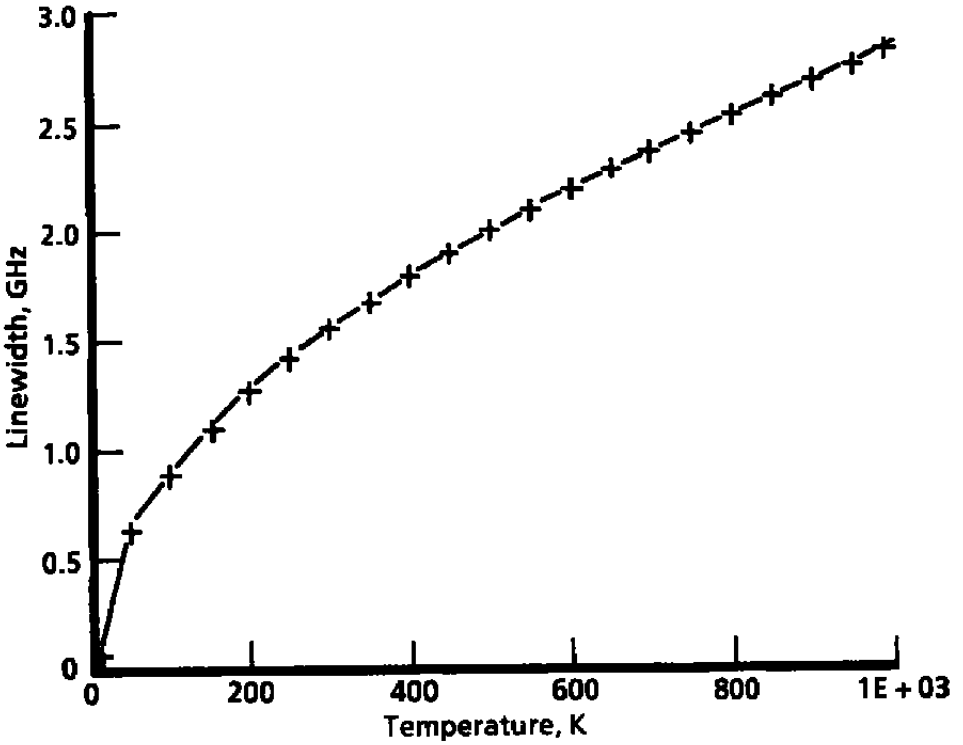

Figure 3. Sodium linewidth versus temperature.

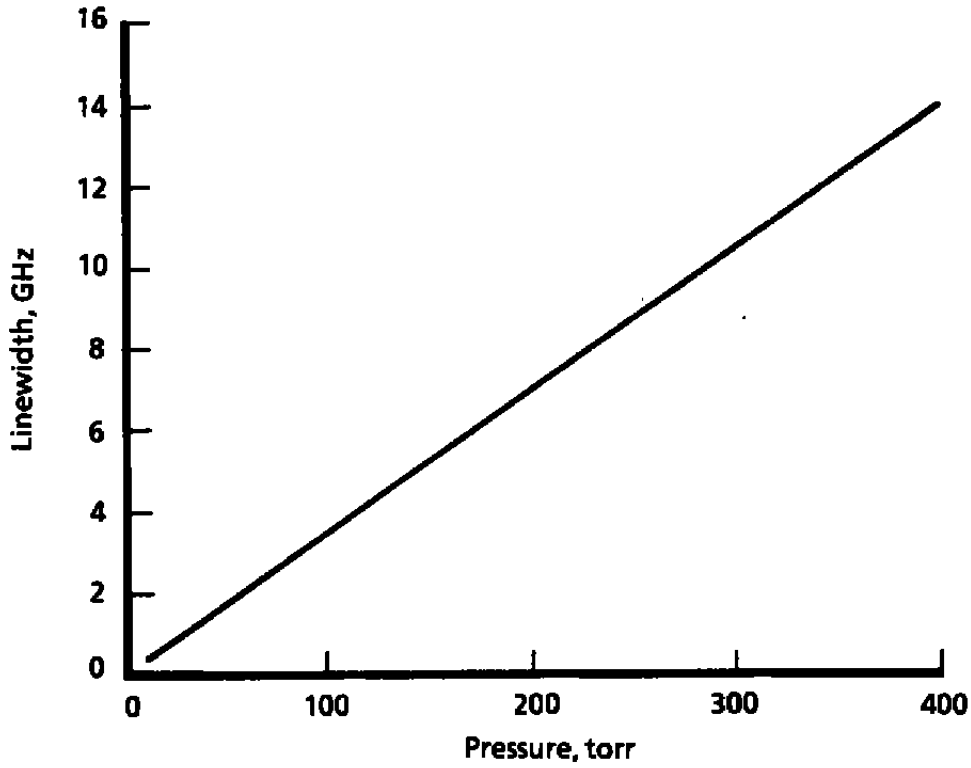

Figure 4. Sodium linewidth versus pressure.

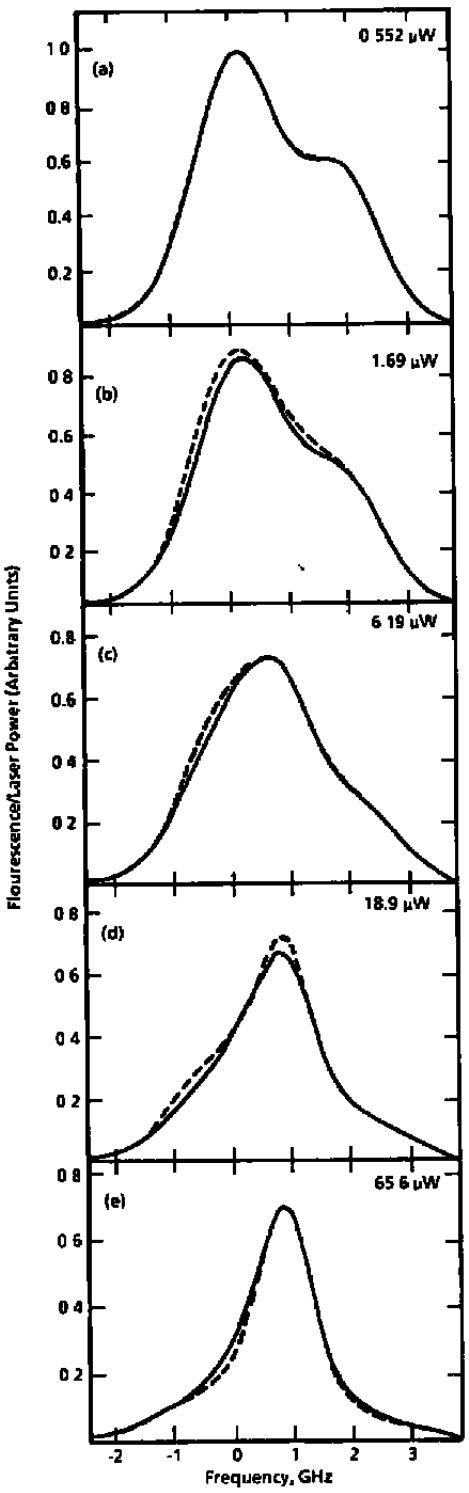

Figure 5. Lineshape distortion due to optical pumping.

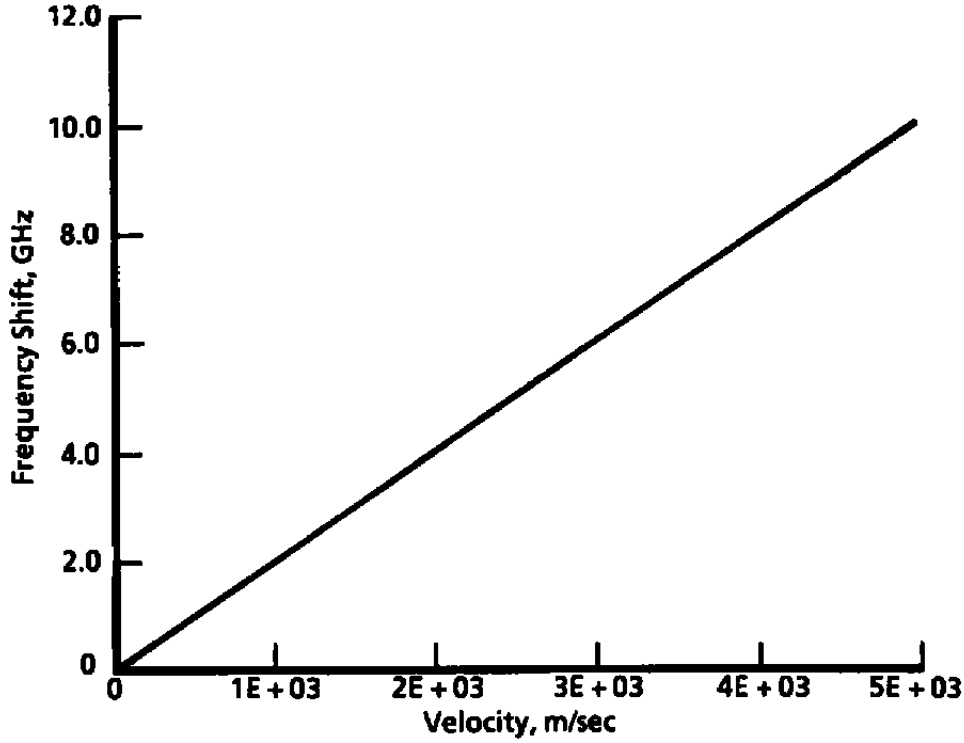

Figure 6. Frequency shift versus gas velocity.

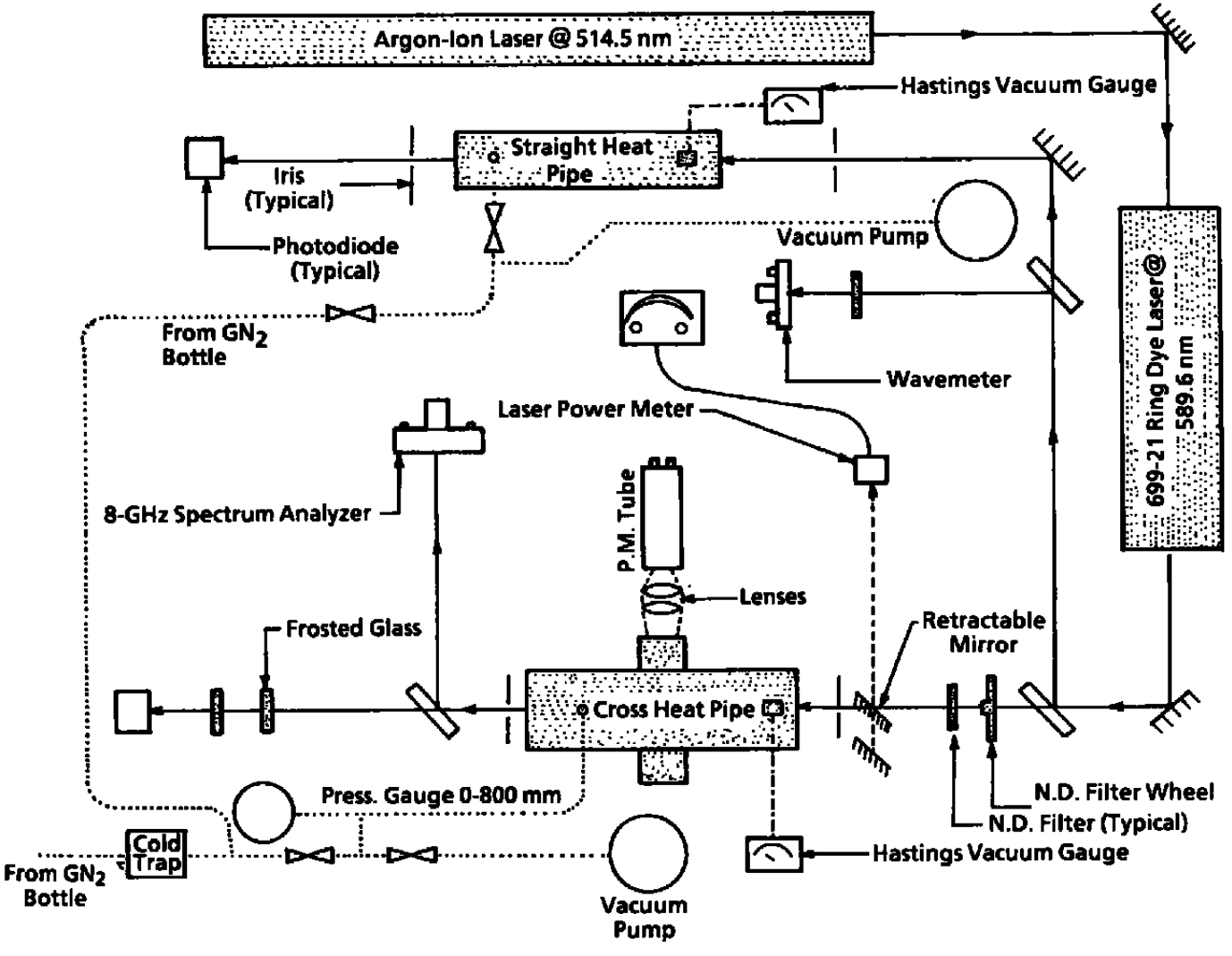

Figure 7. Experimental setup.

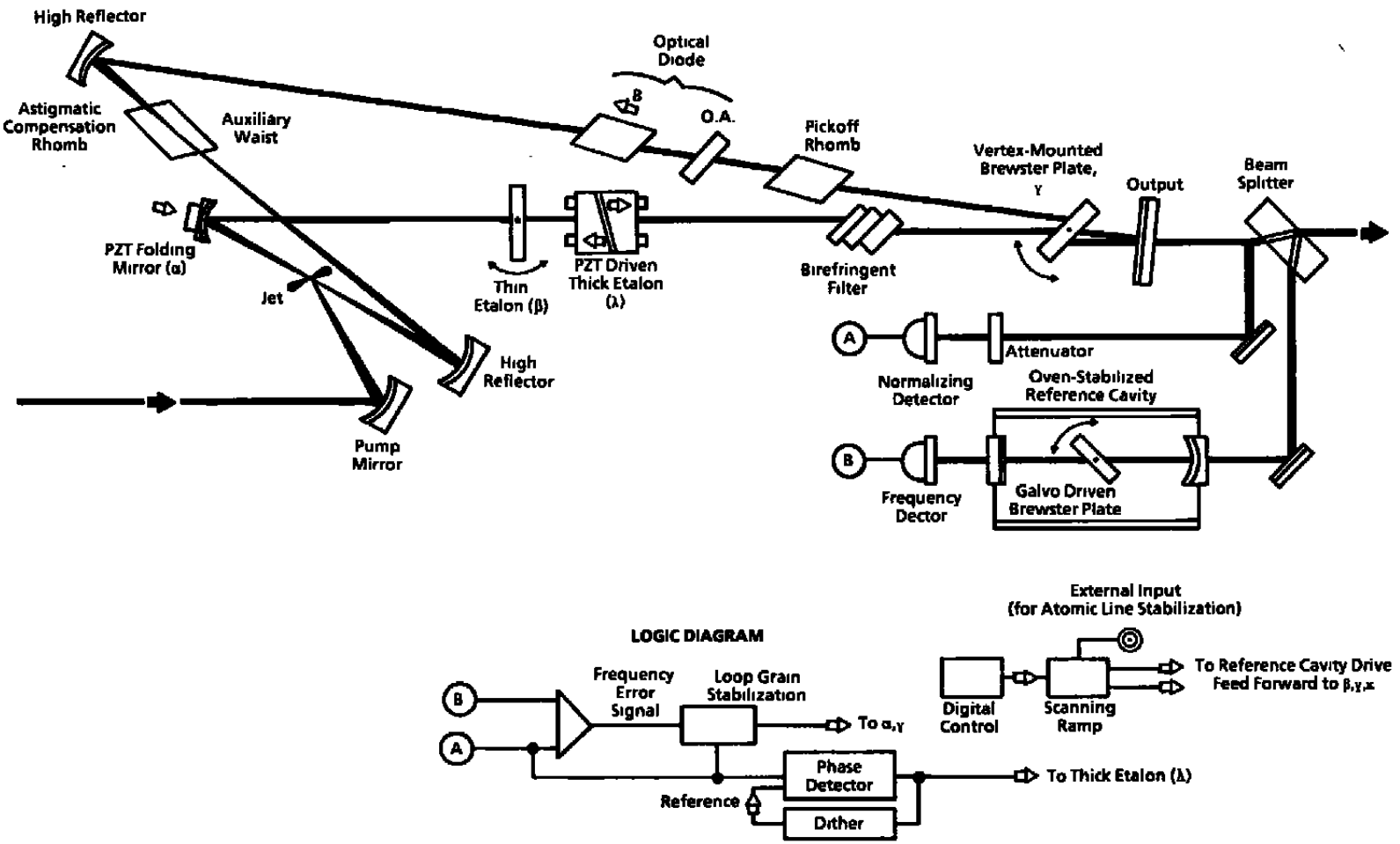

Figure 8. Ring laser cavity.

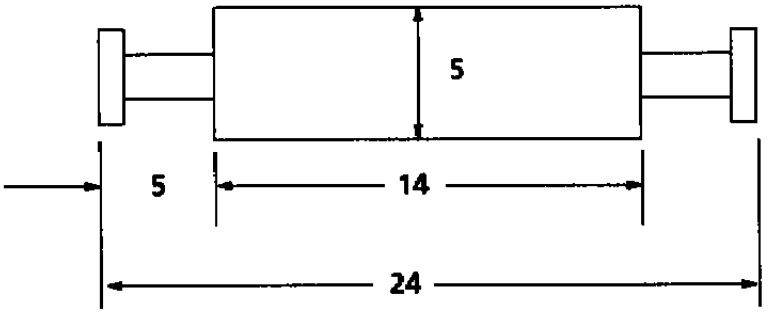

All Dimensions in Inches

Figure 9. In-line reference cell.

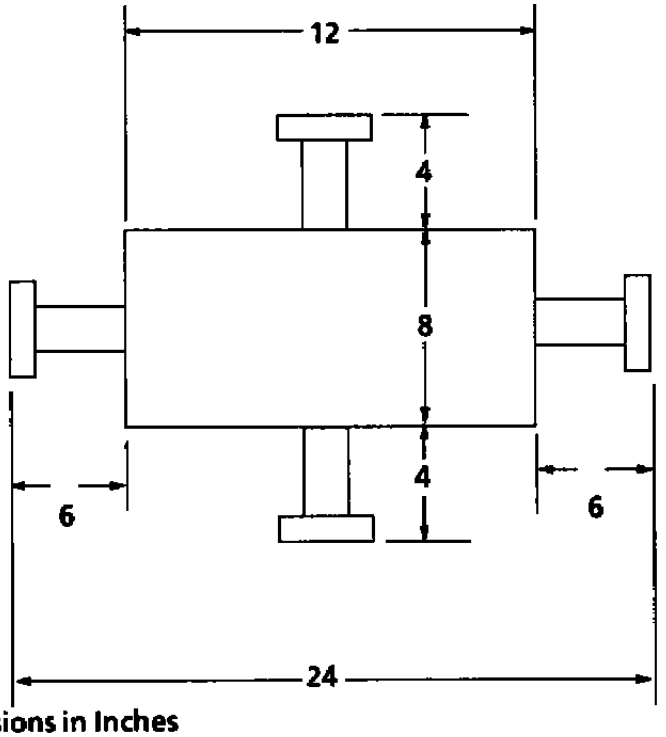

All Dimensions in Inches

Figure 10. Cross-vapor cell.

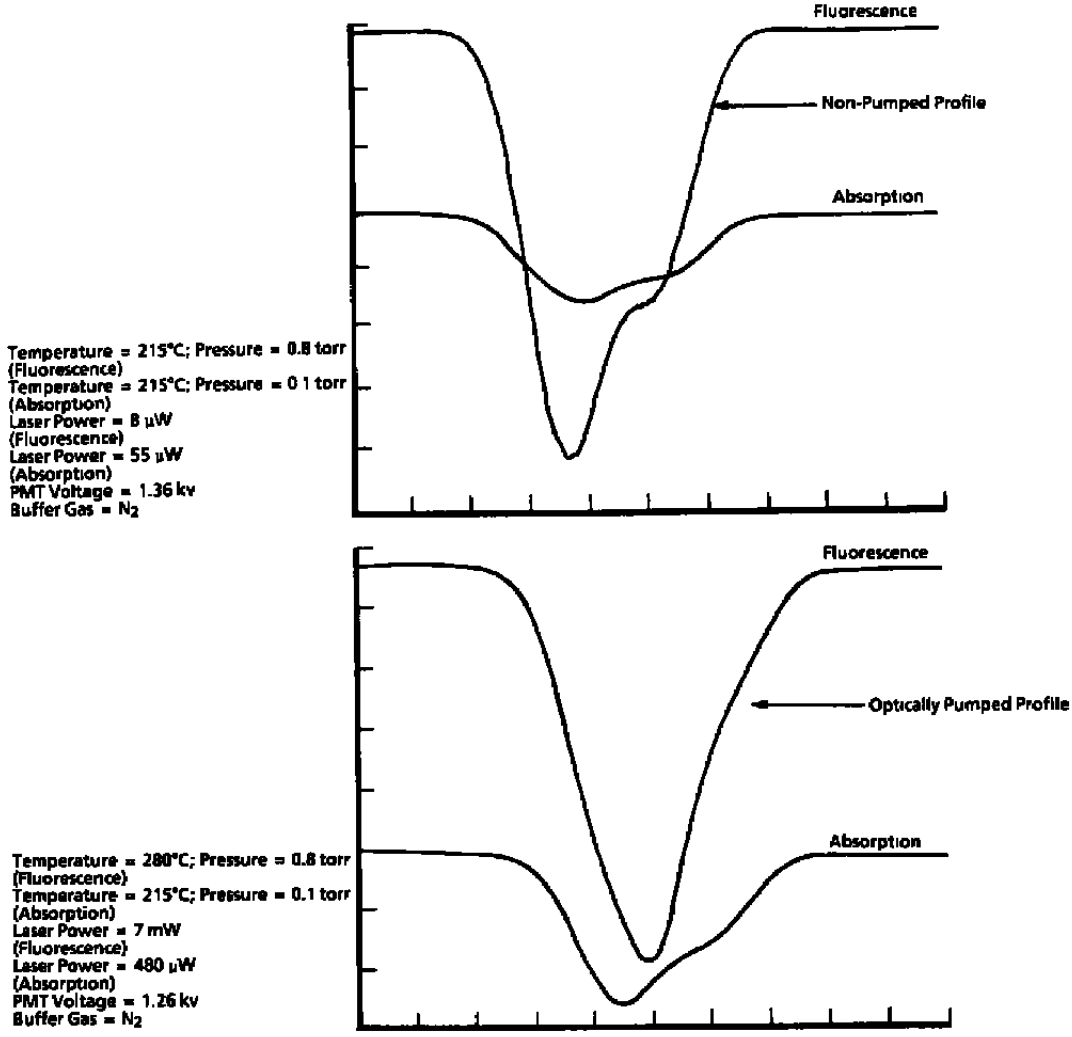

Figure 11. Experimental lineshape with optical pumping.

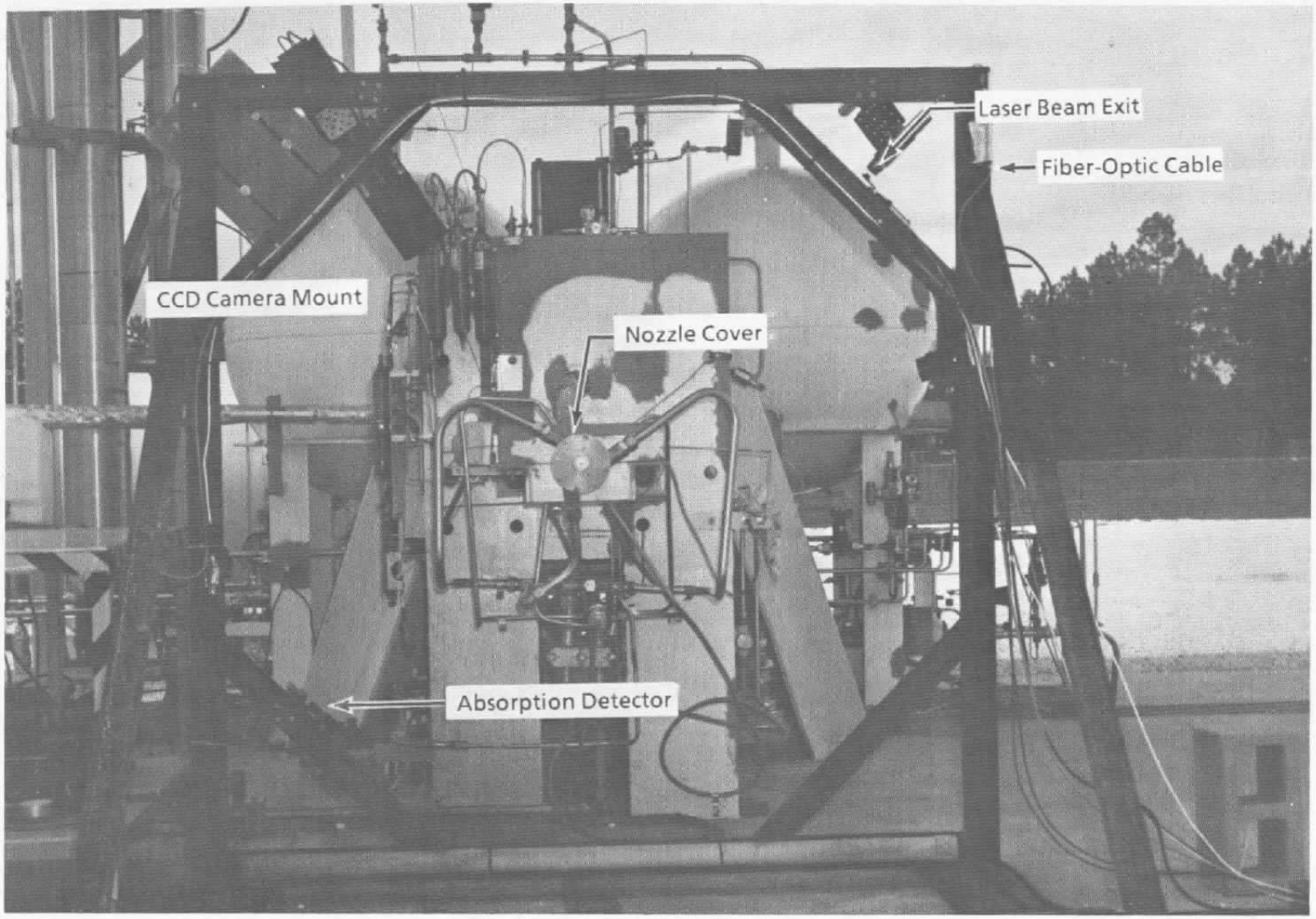

Figure 12. Photograph of diagnostic test facility.

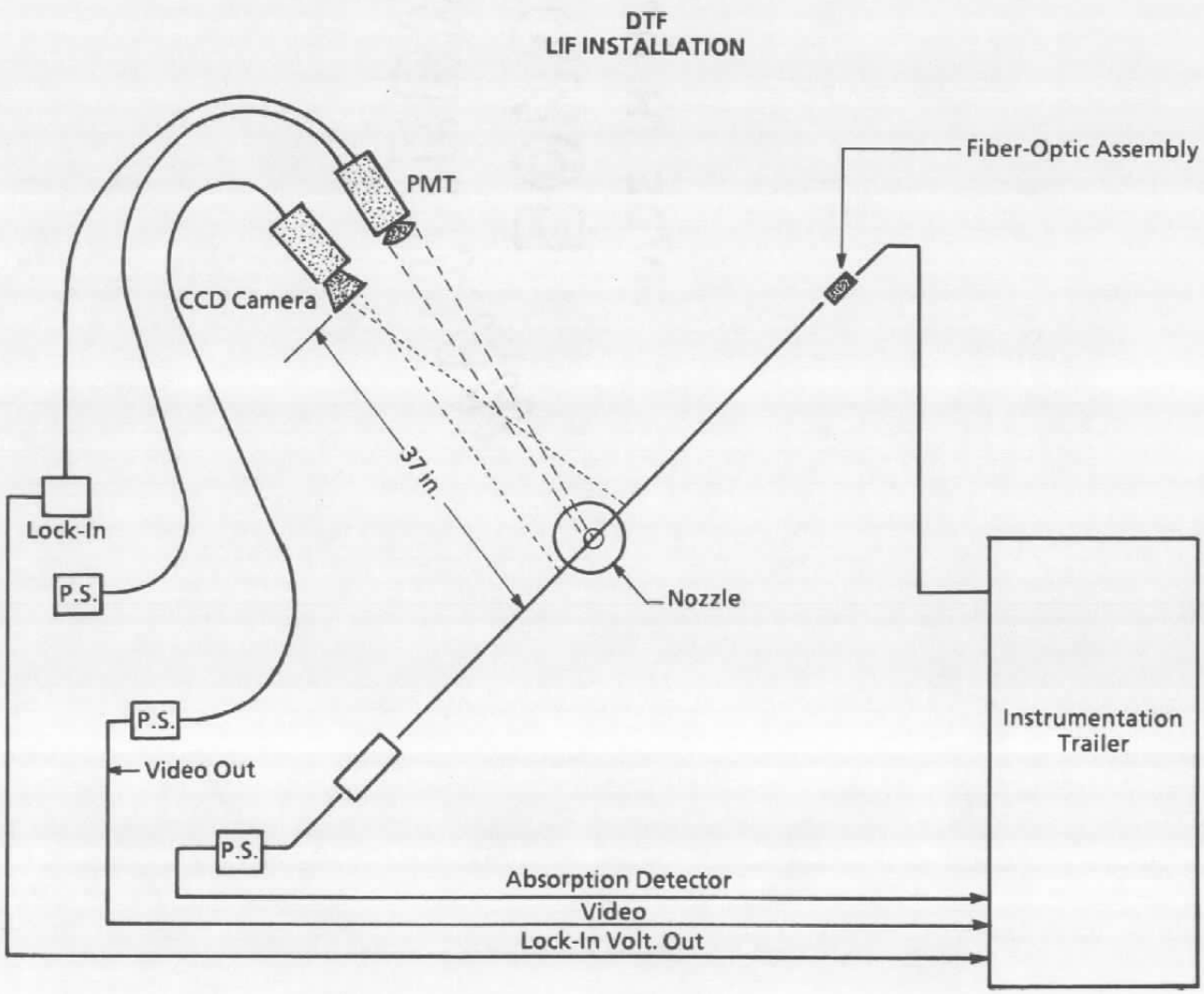

Figure 13. Schematic of diagnostic test facility layout.

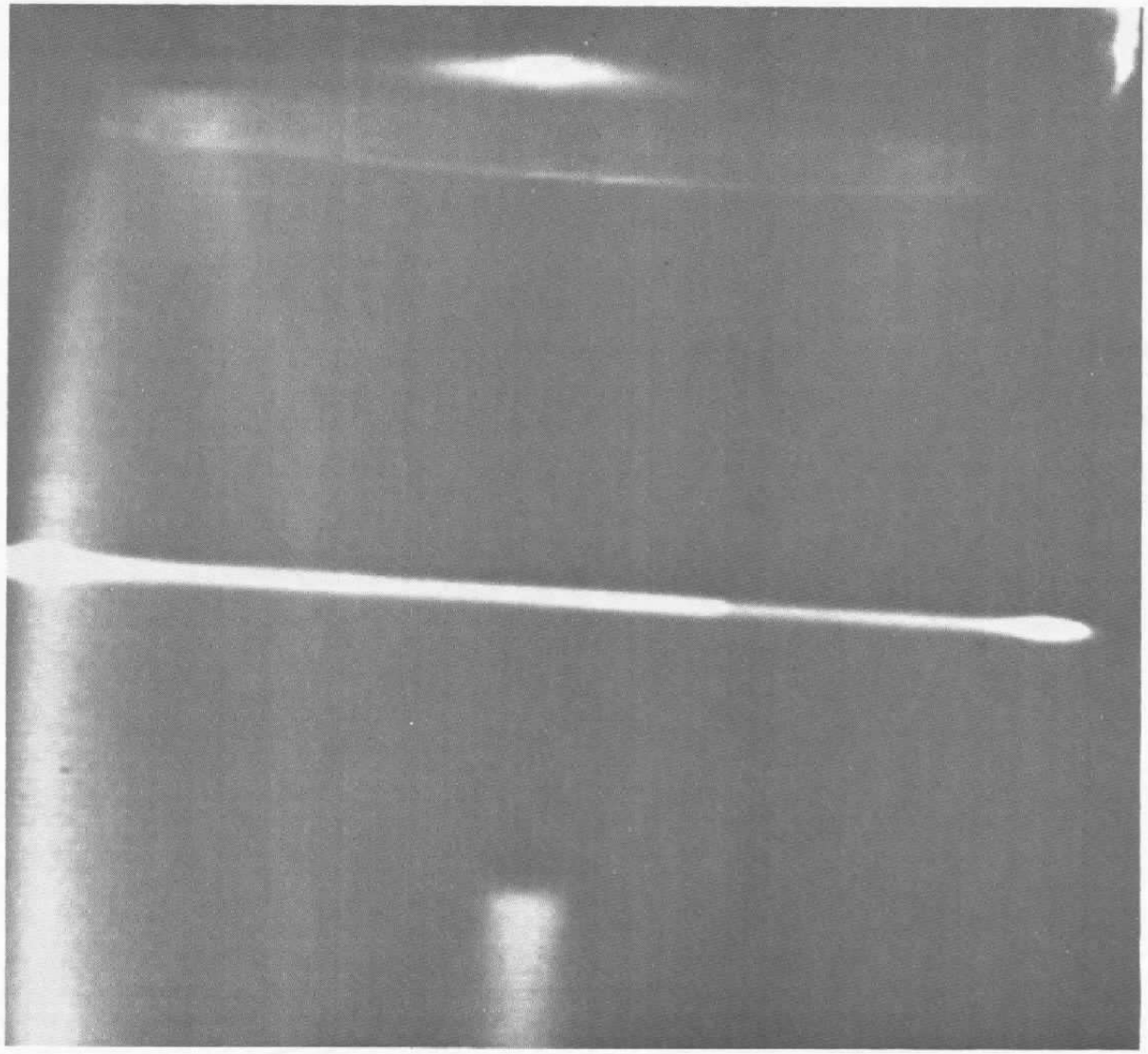

Figure 14. Photograph of video image of sodium fluorescence in DTF plume.

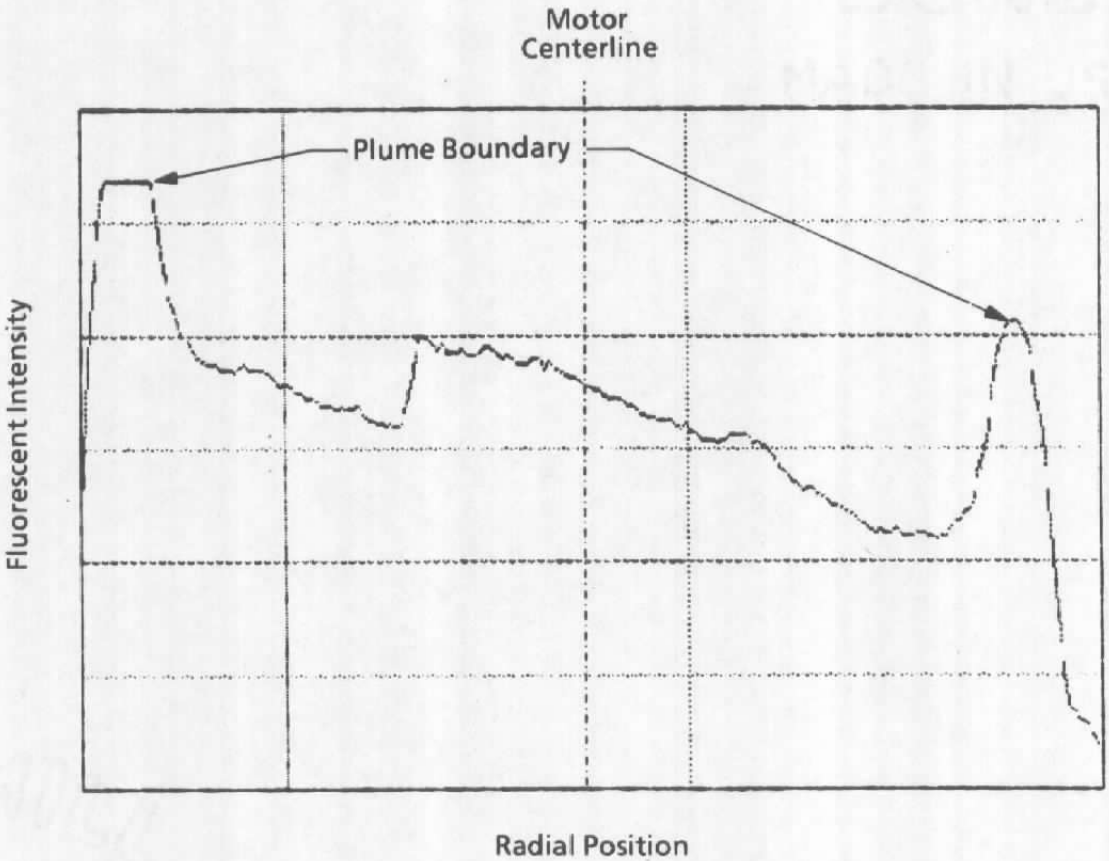

Figure 15. Fluorescence profile at axial position of 1.5 in.

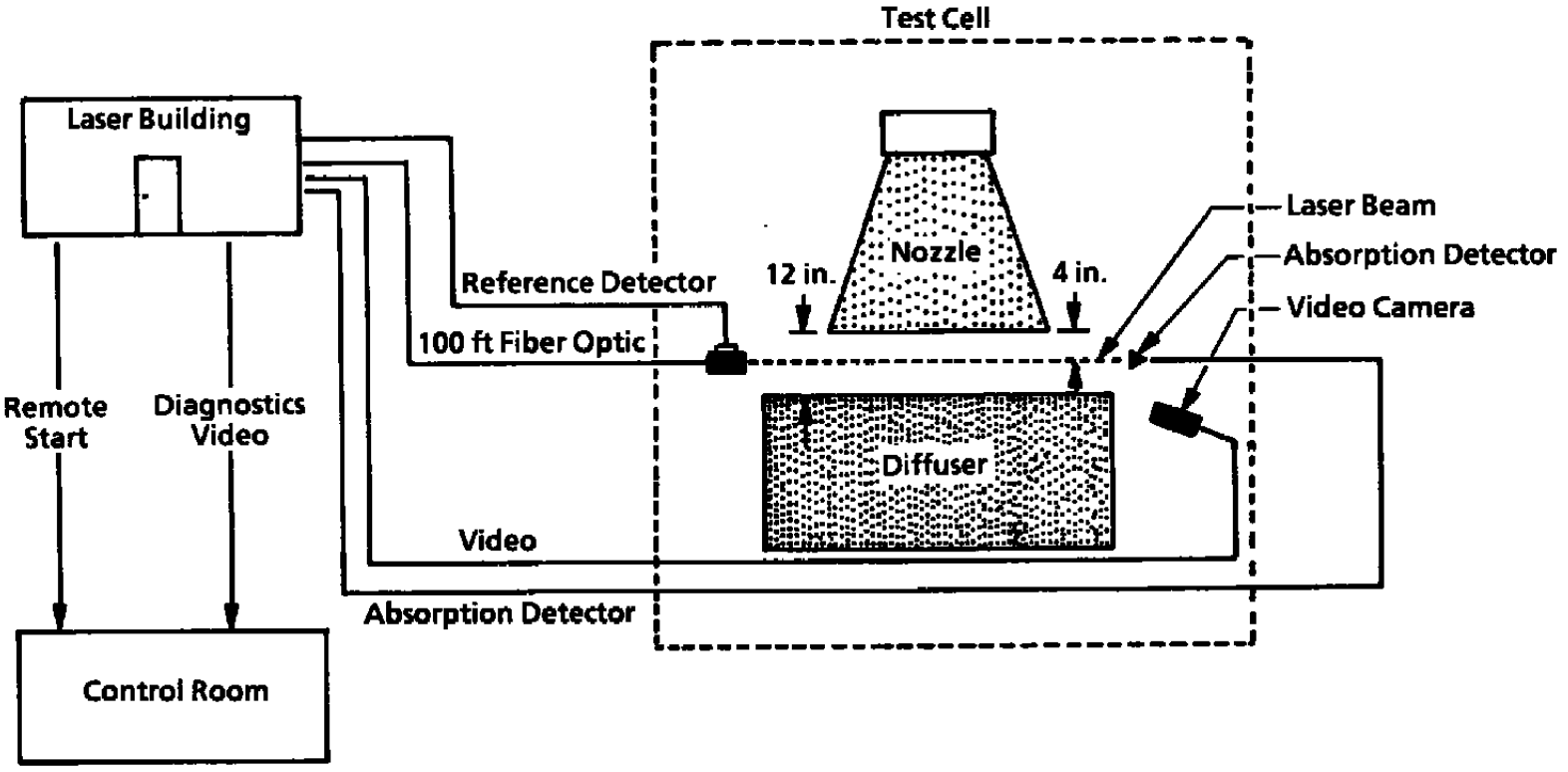

a. OMS LIF installation (side view).

Figure 16. OMS LIF installation.

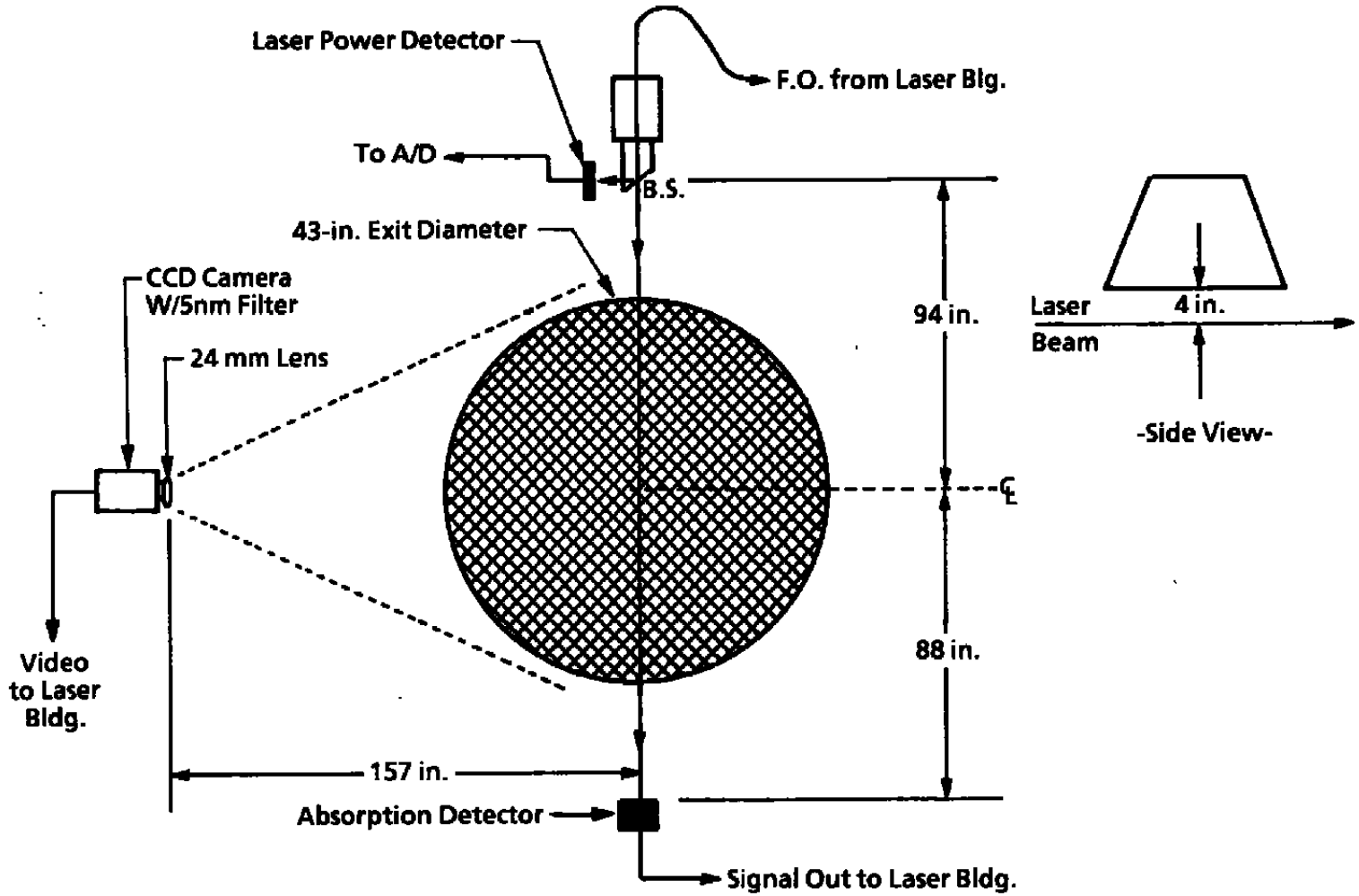

b. OMS LIF installation (top view).

Figure 16. Concluded.

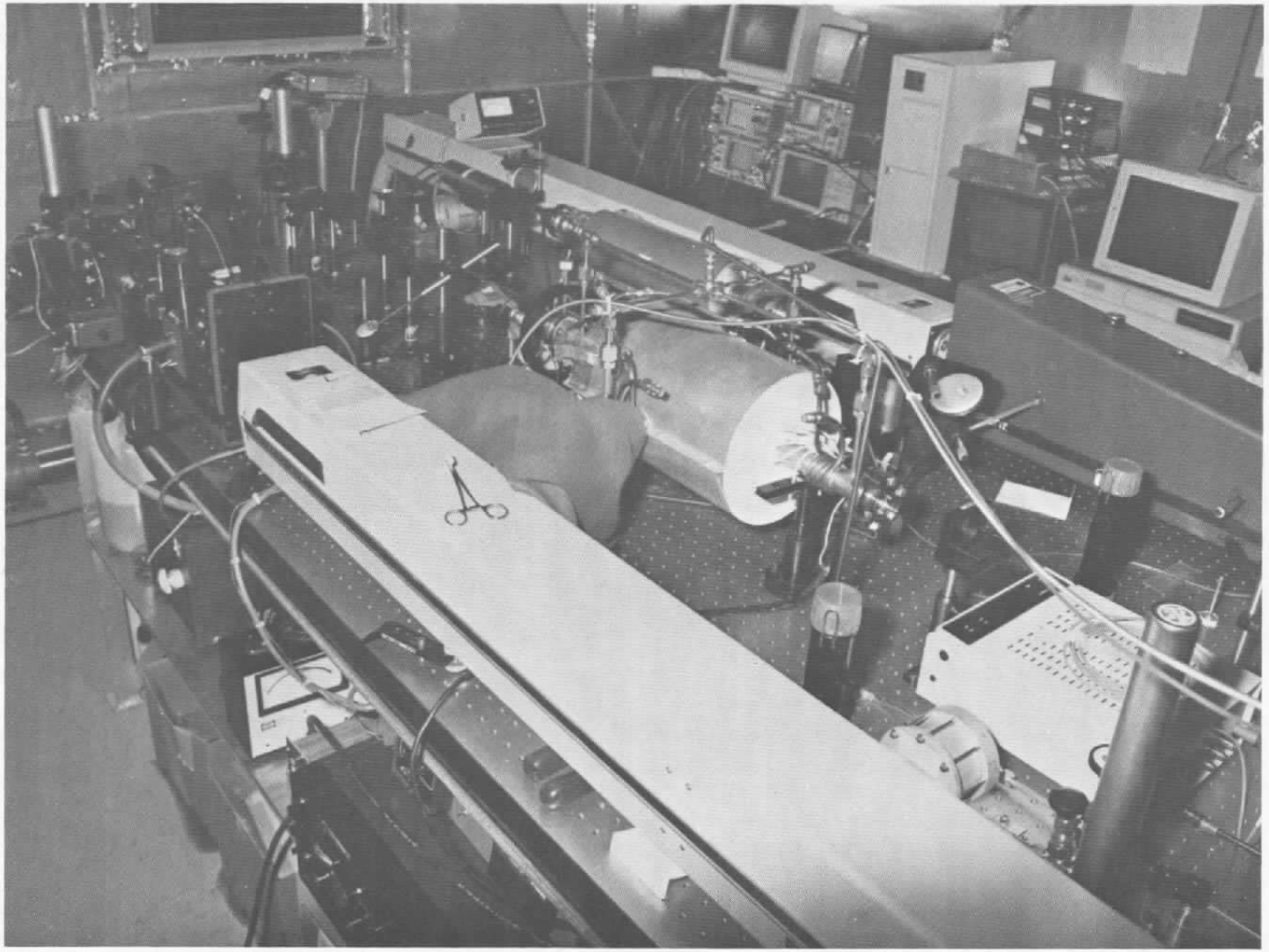

Figure 17. Photograph of OMS laser system setup.

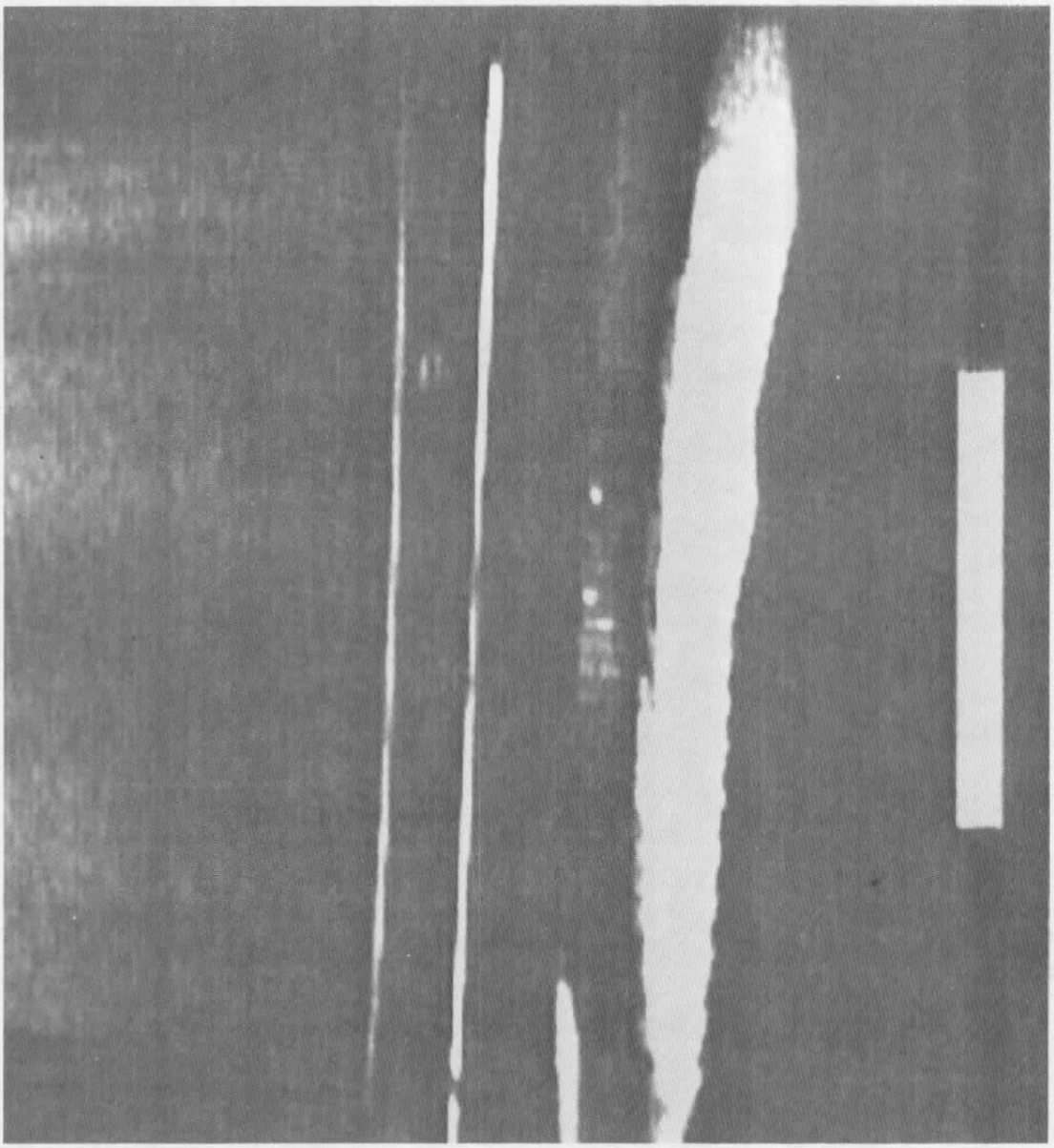

Figure 18. Photograph of video image of sodium fluorescence in OMS plume.

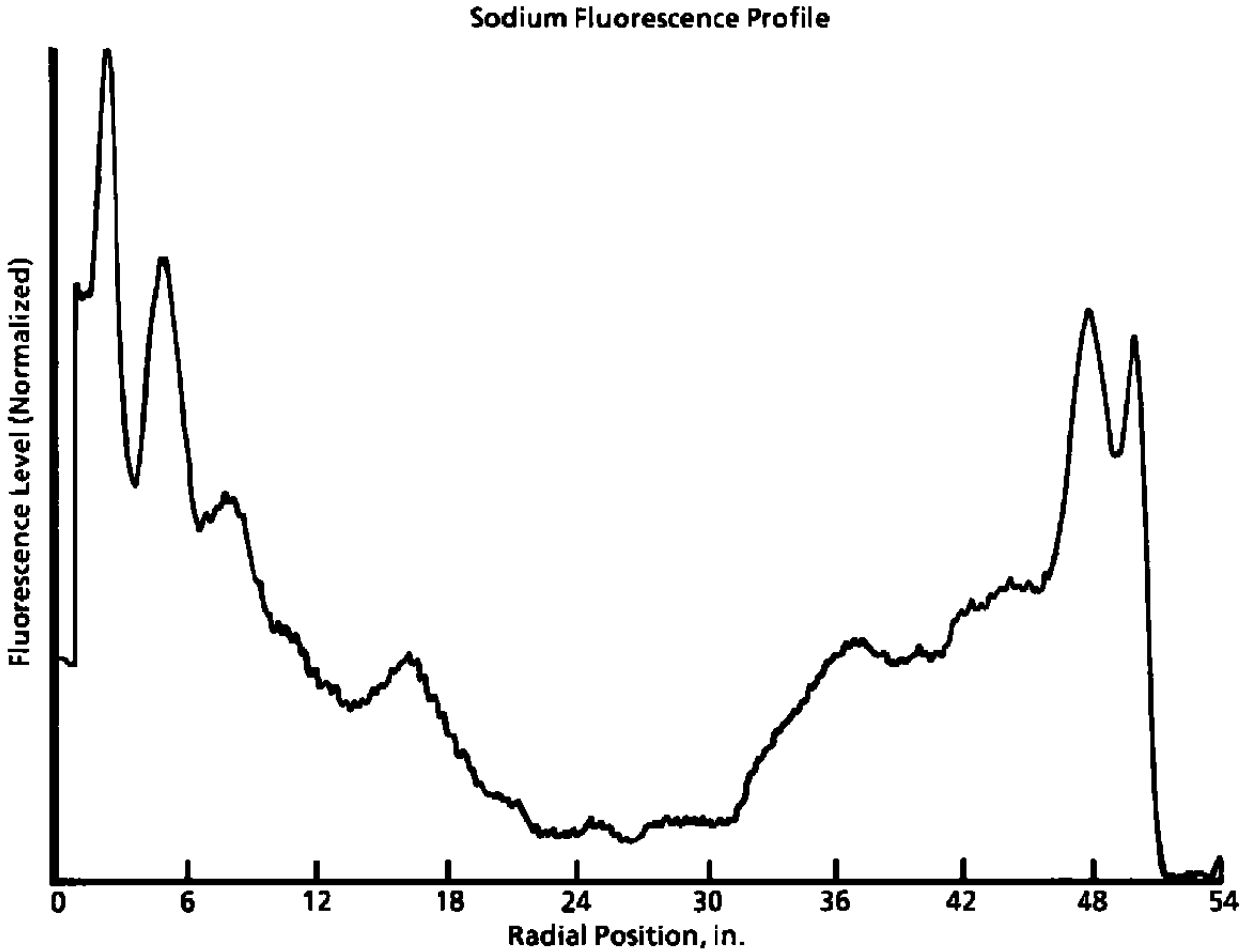

Figure 19. Sodium fluorescence distribution in OMS plume.

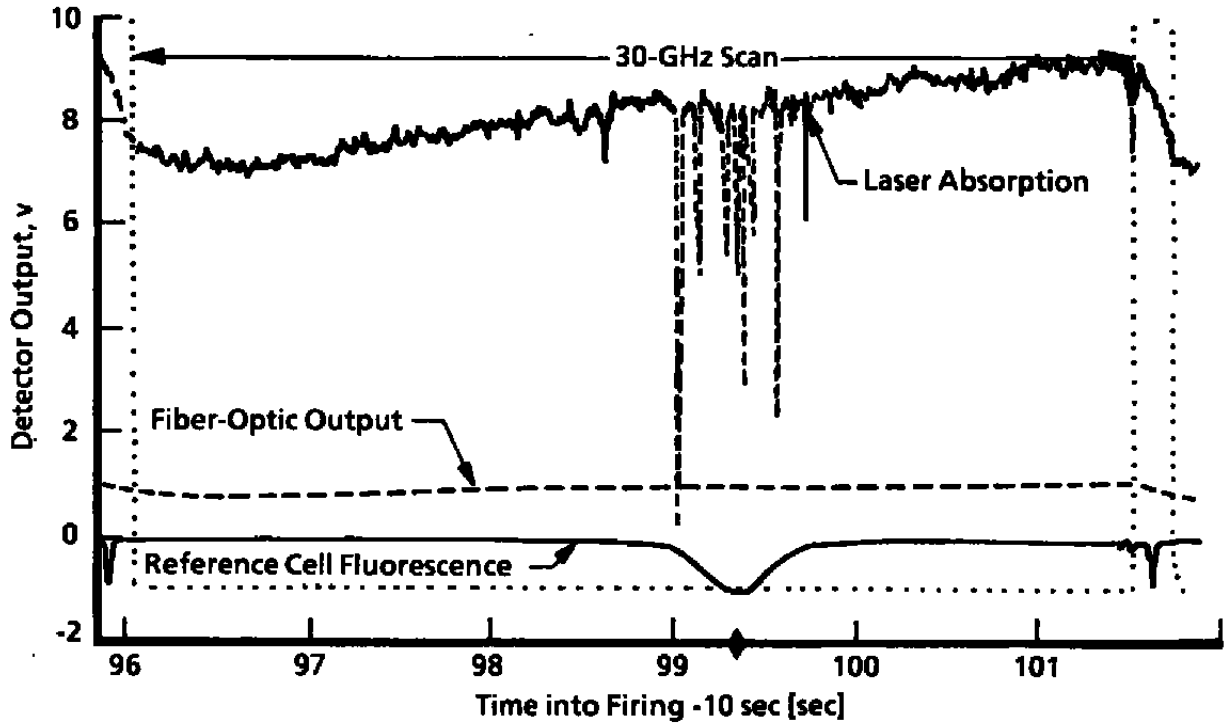

Figure 20. Laser absorption and references.

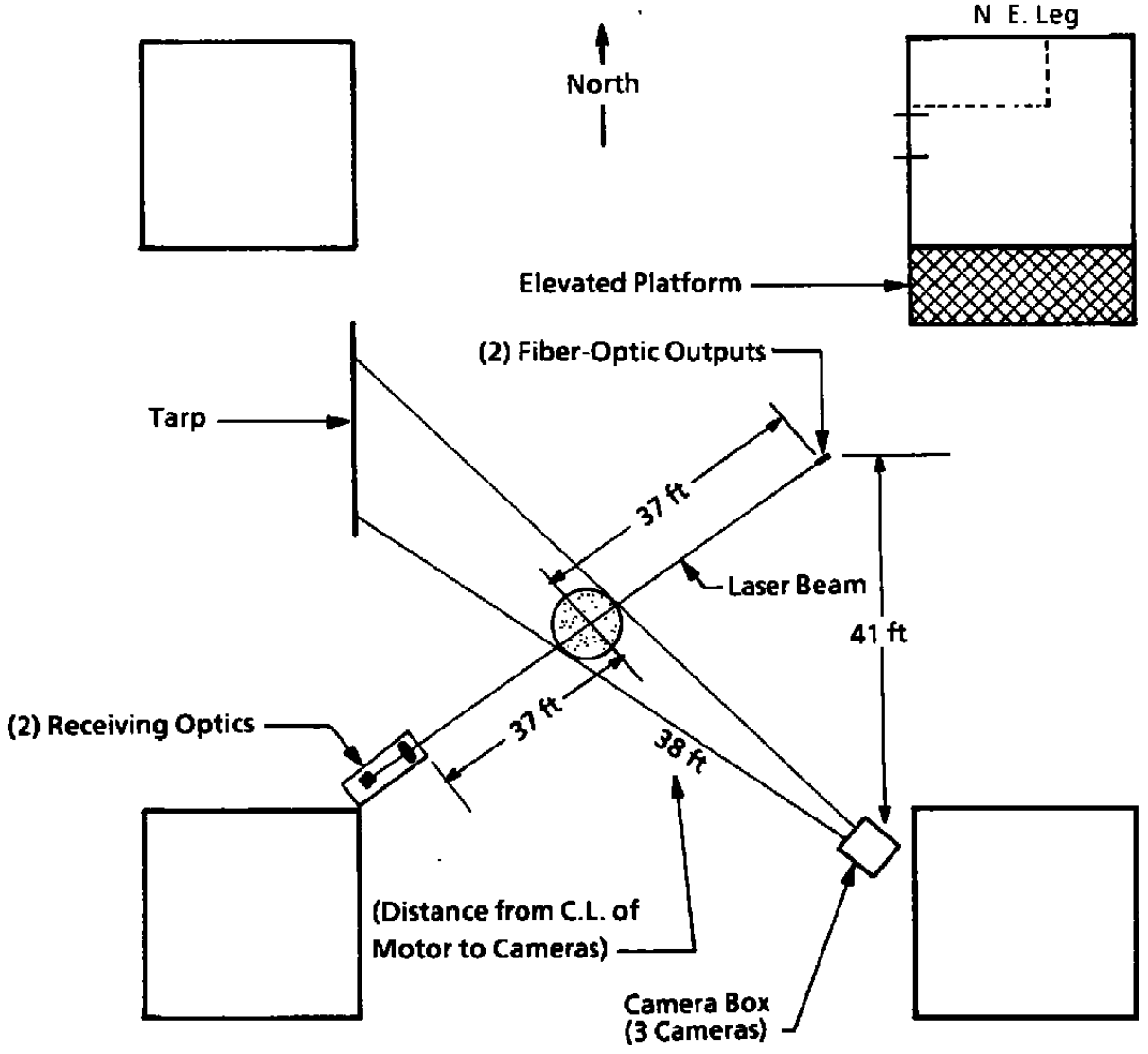

Figure 21. SSME deck area LIF system installation.

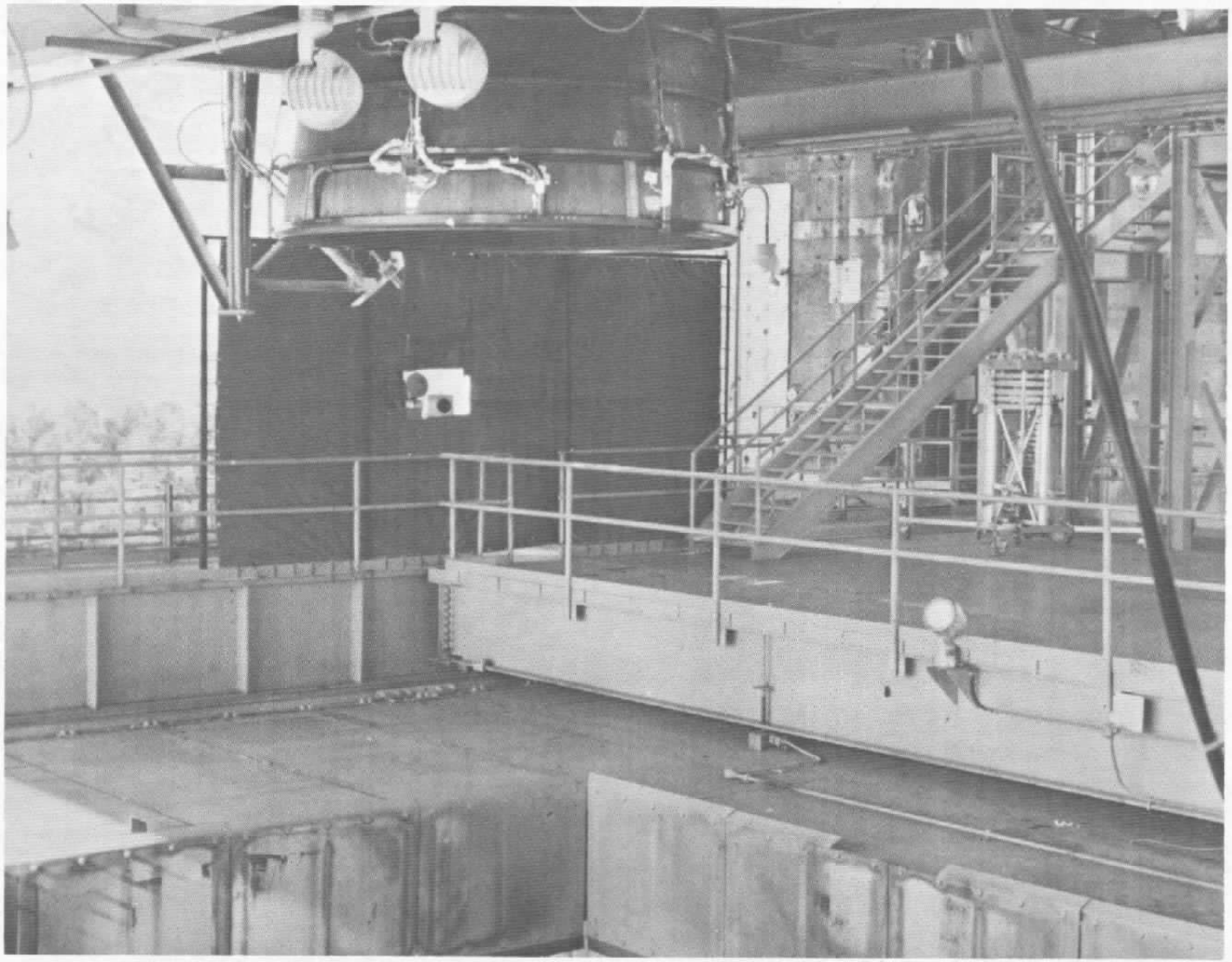

Figure 22. Photograph of Level 10 area.

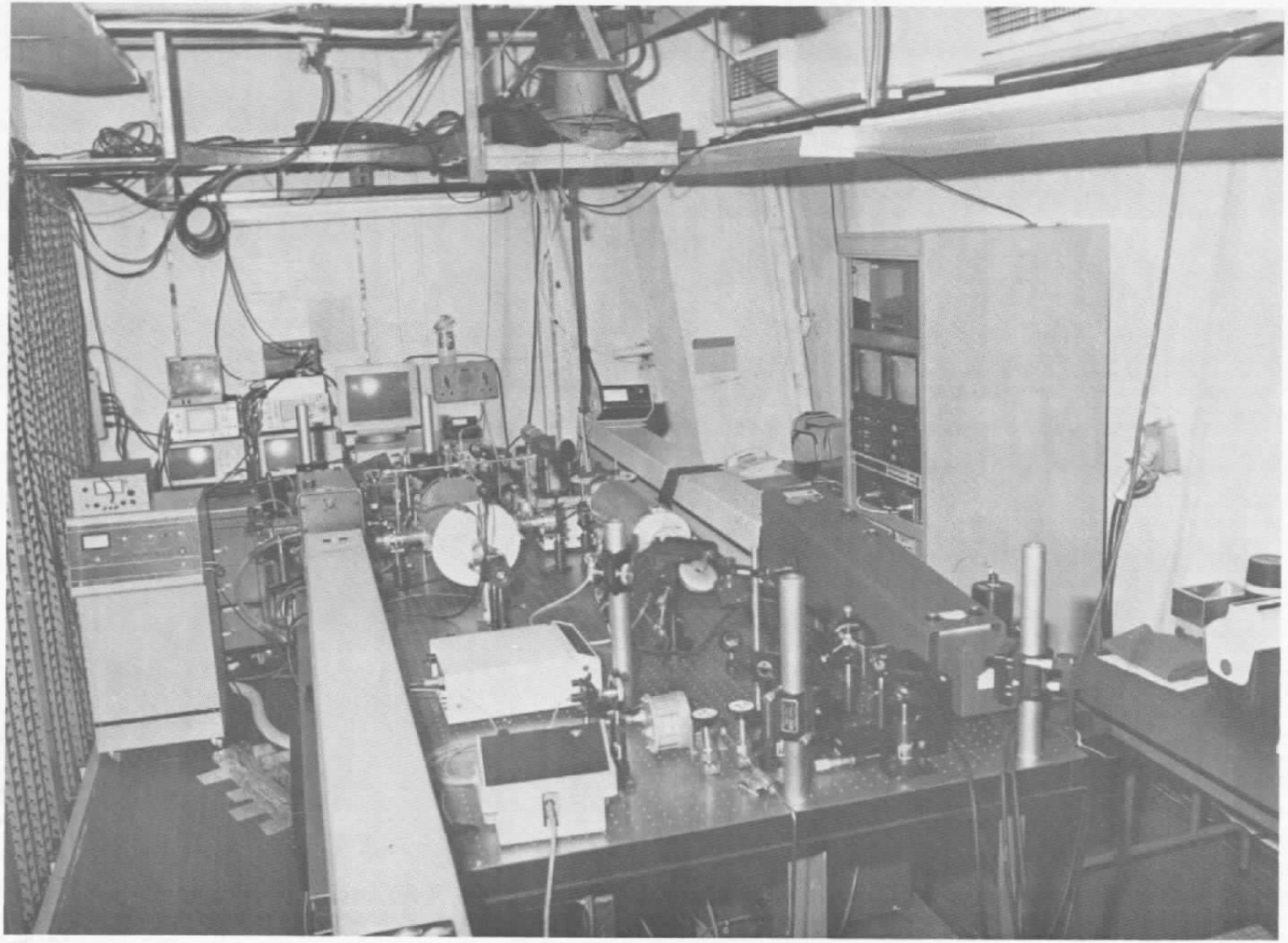

Figure 23. Photograph of Level 10 instrument room.

Table 1. Physical and Spectral Properties of Sodium Atoms

Physical Properties of the Sodium Atom

Atomic Weight, gm/mole	22.9898
Melting Point, °C	97.81
Boiling Point, °C	882.9
Electronic Configuration	$1S^2\ 2S^2\ 2P^2\ 3S^1$
Polarizability, 10^{-24} cm^3	23.6
No Natural Isotopes	

Spectral Properties of Sodium D Lines

Natural Linewidth, MHz	9.76 ± 0.3
Life Time, nsec	16.3 ± 0.5
Resonance Wavelength, Å	
D_1 Line	5896
D_2 Line	5890
Oscillator Strength	
D_1 Line	0.33
D_2 Line	0.65

Sodium Vapor Pressure

T, °C	P, torr
127	2.2×10^{-6}
227	1.15×10^{-3}
327	5.02×10^{-2}
427	0.888
527	7.53
627	39.98
727	148.5
827	453.7

Table 2. DTF LIF System Specifications

Pump Laser	Spectra Physics 171-09 operating at 7.0 W and 0.5145 μm
Dye Laser	Coherent 699-21 scanning ring-dye
Dye	Rhodamine 6G
Dye Laser Linewidth	less than 500 KHz
Center Wavelength	0.5896 μm
Laser Power	70 mW
Scan Range	30 GHz
Scan Rate	1 scan per 6 sec
Fiber Optic	Single mode
Beam Diameter	2.0 mm
Axial Beam Position	1.5 in. from exit plane

Data Acquisition:
Beam Transmission through Plume
Reference Cell Fluorescence
Laser Scan Widths via Laser Blanking
Data Rate: 500 Hz per Channel
Camera output on VHS Videotape

LIF Visualization:
Video Camera: Sony XC-77 with Na line filter
Field of View: 4 in.
Note: Line filters are 5-nm HWHM

Table 3. OMS LIF System Specifications

System #1:	Pump Laser	Spectra Physics 171-09 operating at 7.0 W and 0.5145 μm
	Dye Laser	Coherent 699-21 scanning ring-dye
	Dye	Rhodamine 6G
	Dye Laser Linewidth	less than 500 KHz
	Center Wavelength	0.5896 μm
	Laser Power	80 mW
	Scan Range	30 GHz
	Scan Rate	1 scan per 6 sec
	Fiber Optic	Single mode
	Beam Diameter	3.0 mm
	Axial Beam Position	4 in. from exit plane
System #2:	Same as #1 with exception of the following:	
	Fiber Optic	Single mode
	Beam Diameter	3.0 mm
	Axial Beam Position	4 in. from exit plane

Data Acquisition (Both Systems):
- Fiber-Optic Output Power
- Beam Transmission through Plume
- Reference Cell Fluorescence
- Laser Scan Widths via Laser Blanking
- Data Rate at 500 Hz per channel
- Camera Output on VHS Tape

LIF Visualization (Video Cameras):
- 1 Dage CCD with line filter—54-in. field of view
- 1 Xybion with line filter—54-in. field of view
- Note: Line filters are 5-nm HWHM

Table 4. SSME LIF System Specifications.

System #1:	Pump Laser	Spectra Physics 171-09 operating at 7.0 W and 0.5145 μm
	Dye Laser	Coherent 699-21 scanning ring-dye
	Dye	Rhodamine 6G
	Dye Laser Linewidth	less than 500 KHz
	Center Wavelength	0.5896 μm
	Laser Power	80 mW
	Scan Frequency	30 GHz
	Scan Range	1 scan per 6 sec
	Fiber Optic	Single mode
	Beam Diameter	1.5 in.
	Axial Beam Position	3.5 in. from exit plane
System #2:	Same as #1 with exception of the following:	
	Fiber Optic	Multi-mode
	Beam Diameter	2.0 in.
	Axial Beam Position	13.5 in. from exit plane

Data Acquisition (Both Systems):
- Fiber-Optic Output Power
- Beam Transmission through Plume
- Reference Cell Fluorescence
- Laser Scan Widths via Laser Blanking
- Data Rate at 500 Hz per channel
- Camera Output on VHS Videotape

LIF Visualization (Video Cameras):
- 1 Dage CCD with line filter—96-in. field of view
- 1 RCA SIT with line filter—96-in. field of view
- 1 Xybion with line filter—48-in. field of view
- Note: Line filters are 5-nm HWHM